

AD-A013 855

ROLE OF FERRIC OXIDE SURFACE AREA  
IN PROPELLANT BURN RATE ENHANCEMENT  
(FIRST STEP TOWARD MODELING)

C. H. Burnside

Rockwell International Corporation

Prepared for:

Air Force Office of Scientific Research

30 June 1975

DISTRIBUTED BY:

**NTIS**

National Technical Information Service  
U. S. DEPARTMENT OF COMMERCE

UNCLASSIFIED 30JUL75

SECURITY CLASSIFICATION OF THIS PAGE (When Data Entered)

REPORT DOCUMENTATION PAGE		READ INSTRUCTIONS BEFORE COMPLETING FORM
1. REPORT NUMBER AFOSR - TR - 75 - 1126	2. GOVT ACCESSION NO.	3. RECIPIENT'S CATALOG NUMBER AD-A 013 155
4. TITLE (and Subtitle) ROLE OF FERRIC OXIDE SURFACE AREA IN PROPELLANT BURN RATE ENHANCEMENT (FIRST STEP TOWARD MODELING)	5. TYPE OF REPORT & PERIOD COVERED Final. 1JUL74 through 30JUN75	
	6. PERFORMING ORG. REPORT NUMBER K-4889	
7. AUTHOR(s) C. H. Burnside	8. CONTRACT OR GRANT NUMBER(s) F44620-75-C-0002	
9. PERFORMING ORGANIZATION NAME AND ADDRESS Rocketdyne Division Rockwell International Corporation P.O. Box 548, McGregor, TX 76657	10. PROGRAM ELEMENT, PROJECT, TASK AREA & WORK UNIT NUMBERS 681308 9711-01 61102F	
11. CONTROLLING OFFICE NAME AND ADDRESS Air Force Office of Scientific Research /NA 1400 Wilson Blvd. Arlington, VA 22209	12. REPORT DATE 30JUN75	
	13. NUMBER OF PAGES 56	
14. MONITORING AGENCY NAME & ADDRESS (if different from Controlling Office)	15. SECURITY CLASS. (of this report)  UNCLASSIFIED	
	15a. DECLASSIFICATION, DOWNGRADING SCHEDULE	
16. DISTRIBUTION STATEMENT (of this Report)  Approved for public release; distribution unlimited.		
17. DISTRIBUTION STATEMENT (of the abstract entered in Block 20, if different from Report)		
18. SUPPLEMENTARY NOTES		
19. KEY WORDS (Continue on reverse side if necessary and identify by block number)  SOLID ROCKET PROPELLANTS; SURFACES; IRON COMPOUNDS; OXIDES; CATALYSTS; BURNING RATE; MODELS		
20. ABSTRACT (Continue on reverse side if necessary and identify by block number)  Results of efforts to correlate composite propellant burn rate, ammonium perchlorate particle size distribution, and ferric oxide specific surface and level are presented. Results from laboratory-scale motor firings with HTPB- and CTPB-based propellants containing ferric oxides of 3 to 26.4 m <sup>2</sup> /gm were used. The oxides had been prepared by precipitation and by calcination of either ferric sulfate or yellow iron oxide. Outcome of the analysis is a quantitative summarization of a mass of data showing how the several oxides -- continued --		

DD FORM 1 JAN 73 1473

EDITION OF 1 NOV 65 IS OBSOLETE

UNCLASSIFIED

SECURITY CLASSIFICATION OF THIS PAGE (When Data Entered)

perform in terms of their specific surface and level and as a function of oxidizer particle size distribution.

Results indicate  $\text{Fe}_2\text{O}_3$  specific surface is more significant at high fine-AP levels than at low fine-AP levels. They also indicate that at a given weight level  $\text{Fe}_2\text{O}_3$  with a high specific surface is a better catalyst than a low specific surface counterpart and that this catalytic effectiveness is not only reflected in burn rate but also as an increase in pressure exponent. Catalytic activity appears to be a function of pressure.

Efforts to utilize the correlations in combustion modeling have barely begun. Catalysis probably takes place in the primary diffusion flame located at the AP-binder interface. Kinetics of this flame are, in the non-catalyzed case, represented by a simple power function in pressure. Results of the correlation analysis indicate that either a slightly modified power function kinetic form or a kinetic model based on reaction between a gas molecule and an adsorbed molecule might describe the behavior of  $\text{Fe}_2\text{O}_3$  catalysts in composite propellants.

1a  
UNCLASSIFIED

SECURITY CLASSIFICATION OF THIS PAGE(When Data Entered)



**Rocketdyne Division**  
**Rockwell International**

P.O. Box 548  
McGregor, Texas 76657

R-4889  
75RT0640  
Enc. 1

SCIENTIFIC REPORT  
ROLE OF FERRIC OXIDE SURFACE AREA  
IN PROPELLANT BURN RATE ENHANCEMENT  
(FIRST STEP TOWARD MODELING)

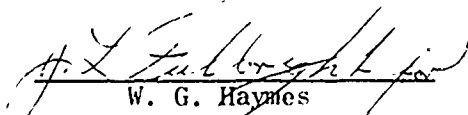
Submitted to Combustion Energetics Division, AFOSR

30 June 1975

Work performed under sponsorship of  
Combustion Energetics Division of  
Air Force Office of Scientific Research,  
Contract F44620-75-C-0002

Prepared by  
C. H. Burnside  
Principal Investigator  
Member Technical Staff

Approved by

  
W. G. Haymes  
Chief Engineer  
Engineering

  
B. M. Corley  
Manager  
Materials

DDC  
RECEIVED  
AUG 19 1975  
RECEIVED  
B

Approved for public release;  
distribution unlimited.



Rocketdyne Division  
Rockwell International

#### FOREWORD

This report contains results of effort carried out under Contract F44620-75-C-0002 directed toward incorporation of ferric oxide catalysis into the competing-flame combustion model. Lloyd R. Lawrence, Jr., Captain, USAF, of the Air Force Office of Scientific Research was program monitor.



## CONTENTS

Introduction. . . . .	1
Experimental Background for Correlation . . . . .	5
General Propellant Compositions . . . . .	5
Ferric Oxide Characteristics. . . . .	5
Specific Propellants. . . . .	5
Correlation: Data-Fit. . . . .	7
Catalyst Parameter. . . . .	7
Data-Summary Equations. . . . .	8
HTPB Bonding Agent Effects. . . . .	18
Correlation: Discussion and Conclusions. . . . .	20
Fe <sub>2</sub> O <sub>3</sub> Surface Area vs Level . . . . .	20
Coarse AP Effects in HTPB Propellant. . . . .	22
Effects of Fe <sub>2</sub> O <sub>3</sub> Specific Surface and Fine AP Level . . . . .	27
Qualitative Considerations for Combustion Modeling. . . . .	
Final Status and Recommendations for Further Study. . . . .	41
References. . . . .	45
<u>Appendix A</u>	
Comparison of Burn Rates Calculated from Regression Analysis with the Experimental Values . . . . .	A-1

## FIGURES

1	Comparison of Burn Rate vs Pressure Calculated from Multiple Linear Regression Analysis with Experimental Data (HTPB Propellants/No Fe <sub>2</sub> O <sub>3</sub> ). . . . .	15
2	Comparison of Burn Rate vs Pressure Calculated from Multiple Linear Regression Analysis with Experimental Data (HTPB Propellants/Fe <sub>2</sub> O <sub>3</sub> ) . . . . .	16
3	Comparison of Burn Rate vs Pressure Calculated from Multiple Linear Regression Analysis with Experimental Data (CTPB Propellants/No Fe <sub>2</sub> O <sub>3</sub> ). . . . .	17
4	Comparison of Burn Rate vs Pressure Calculated from Multiple Linear Regression Analysis with Experimental Data (CTPB Propellants/Fe <sub>2</sub> O <sub>3</sub> ) . . . . .	17



FIGURES  
(Continued)

5	Effect of Low Level $\text{Fe}_2\text{O}_3$ with High Specific Surface and High Level $\text{Fe}_2\text{O}_3$ with Low Specific Surface . . . . .	20
6	Burn Rates of 86% Solids CTPB Propellants Containing (1) No $\text{Fe}_2\text{O}_3$ and (2) 0.2% $\text{Fe}_2\text{O}_3$ . . . . .	21
7	Burn Rates of 86% Solids CTPB Propellants Containing 0.2% $\text{Fe}_2\text{O}_3$ as Function of Ground AP Size and Level . . . . .	21
8	Burn Rates of 88% Solids HTPB Propellants Containing No $\text{Fe}_2\text{O}_3$ Obtained by By-Rate Substitution in Data-Summary Equations. . . . .	22
9	Burn Rates of 88% Solids HTPB Propellants Containing $\text{Fe}_2\text{O}_3$ Obtained by By-Rate Substitution in Data-Summary Equations. . . . .	25
10	Pattern of Coarse AP Fraction Sizes Used in Obtaining Experimental Data that must be Adhered to in Using Data-Summary Equations for HTPB Propellants. . . . .	24
11	Burn Rates of 88% Solids HTPB Propellants With and Without $\text{Fe}_2\text{O}_3$ Obtained Using Coarse AP Size From Fig. 10 as Inputs to Data-Summary Equations. . . . .	25
12	Comparison of Expected Burn Rate vs Pressure for LCA-9047-1 with Experimental Burn Rates. . . . .	26
13	Effect of Ground AP Size and Level and $\text{Fe}_2\text{O}_3$ Specific Surface on Burn Rate of 86% Solids CTPB Propellant . . . . .	27
14	Effect of Ground AP Level and $\text{Fe}_2\text{O}_3$ Specific Surface on Burn Rate of 88% Solids HTPB Propellants. . . . .	28
15	Effectiveness of $\text{Fe}_2\text{O}_3$ Catalysis as Function of Fine AP Level and $\text{Fe}_2\text{O}_3$ Specific Surface (CTPB Propellants) . . .	29
16	Effectiveness of $\text{Fe}_2\text{O}_3$ Catalysis as Function of Fine AP Level and $\text{Fe}_2\text{O}_3$ Specific Surface (HTPB Propellants) . . .	29
17	$\text{Fe}_2\text{O}_3$ Specific Surface Effectiveness Contours at 1000 psia (HTPB Propellants). . . . .	30
18	$\text{Fe}_2\text{O}_3$ Effectiveness as Function of Pressure (CTPB Propellants) . . . . .	31
19	$\text{Fe}_2\text{O}_3$ Effectiveness as Function of Pressure (HTPB Propellants) . . . . .	31
20	$\text{Fe}_2\text{O}_3$ Effectiveness as Function of Pressure (HTPB Propellants) . . . . .	32



FIGURES  
(Continued)

21	Effect of $\text{Fe}_2\text{O}_3$ Specific Surface on Burn Rate and Pressure Exponent (HTPB Propellants) . . . . .	33
22	Effect of $\text{Fe}_2\text{O}_3$ Specific Surface on Burn Rate and Pressure Exponent (CTPB Propellants) . . . . .	33
23	Effect of $\text{Fe}_2\text{O}_3$ on Burn Rate and Pressure Exponent . . . . .	34
24	Reaction Patterns of Bimolecular Reaction Catalyzed by Solid Surfaces. . . . .	37
25	Reaction Pattern of Bimolecular Gas Phase Reaction . . . . .	38
26	Burn Rate Calculated from Multiple-Flame Combustion Model Using Parameter Inputs from Ref. 2 with Primary Flame Rate Constants Varied. . . . .	39
27	Burn Rates Calculated from Multiple-Flame Combustion Model Using Parameter Inputs from Ref. 2 with Average Flame Height Factors Varied. . . . .	40
28	Effect of Particle Size Distribution on Burn Rate. . . . .	42

TABLES

1	Composition of HTPB Propellants Used for Correlation Analysis . . . . .	5
2	Composition of CTPB Propellants Used for Correlation Analysis . . . . .	4
3	Characteristics of Ferric Oxides . . . . .	5
4	Correlations of Catalyst Parameter and Burn Rate: AP Specific Surface $\sim 4000 \text{ cm}^2/\text{gm}$ . . . . .	9
5	Correlations of Catalyst Parameter and Burn Rate: AP Specific Surface $\sim 1520 \text{ cm}^2/\text{gm}$ . . . . .	10
6	Correlations of Catalyst Parameter and Burn Rate: AP Specific Surface $\sim 1520 \text{ cm}^2/\text{gm}$ . . . . .	11
7	Comparison of Calculated and Experimental Burn Rates of HTPB Propellants Containing Different Bonding Agents . . . . .	18
8	Residuals as Function of Coarse AP Fraction. . . . .	23
9	Composition of Burn Rate Pattern Verification Mix. . . . .	26
10	Ferric Oxide Surface Area Effect on Burn Rate and Pressure Exponent. . . . .	32





## INTRODUCTION

A discussion of efforts directed toward the following goal is presented in this final report: incorporation of ferric oxide catalysis into the multiple-flame combustion model (1) (2). To reach this goal, one must start with experimental results to determine (1) which variables are significant, e.g., differences in  $\text{Fe}_2\text{O}_3$  specific surface and level etc., and: (2) what functional dependencies exist among the variables, e.g., burn rate,  $\text{Fe}_2\text{O}_3$  specific surface and level, ammonium perchlorate particle size distributions and pressure. By utilizing results of the basic combustion studies and experience with solid catalysts in the chemical process industries, one can make an a priori selection of the most probable significant variables.

Results of ammonium perchlorate (AP) - binder sandwich combustion studies (3) indicate that burn rate catalysts dispersed in the binder, as they are in practical propellant formulations, promote combustion at the AP-binder interface. An increase in AP-binder interface should, therefore, bring more of the dispersed catalyst into this interfacial area and in so doing provide more catalyst particles to promote chemical reaction.

Although thermodynamic calculations indicate that ferric oxide catalysts are eventually converted to chlorides, their role may still parallel that of heterogeneous catalysts in ordinary chemical reactions. The particles of  $\text{Fe}_2\text{O}_3$  at the AP-binder interface may enter the gas phase mixing and reaction zones as fluidized particles and enhance select chemical processes in this interfacial region by providing an active surface on which these processes can proceed. The extent of active catalytic surface per unit weight of catalyst in this region must obviously be a function of the specific surface of the  $\text{Fe}_2\text{O}_3$  selected as catalyst.



Rocketdyne Division  
Rockwell International

The logic and significance of an AP- $\text{Fe}_2\text{O}_3$  surface area-to-surface area dependence seemed incontestable. And as no quantitative correlation between  $\text{Fe}_2\text{O}_3$  specific surface and extent of AP-binder interface had been established, the first phase of this modeling effort was directed toward obtaining such a correlation. The "curve-fits" to experimental data and pertinent outcomes calculated from these fits are described in the first three sections of this report. The fourth section contains a first look at use of these correlations in incorporating  $\text{Fe}_2\text{O}_3$  catalysis into the Multiple-Flame Combustion Model. The final section contains recommendations for additional work.



## EXPERIMENTAL BACKGROUND FOR CORRELATION

The experience of Rocketdyne and other solid propellant producers was to be used to correlate  $\text{Fe}_2\text{O}_3$  and AP surface areas and pressure and burn rate. Unfortunately reports by others contained no indication of what specific oxides had been used in their burn rate studies. Hence the experimental background used in this correlation analysis has been limited to that available from Rocketdyne efforts.

## GENERAL PROPELLANT COMPOSITIONS

For the analyses, data obtained from hydroxy-terminated polybutadiene (HTPB)-based propellants and carboxy-terminated polybutadiene (CTPB)-based propellants having the general compositions shown in Table 1 and 2, respectively were used.

TABLE 1  
COMPOSITION OF HTPB PROPELLANTS  
USED FOR CORRELATION ANALYSIS

Ingredient, wt %	Controls	Catalyzed
HTPB Binder	11.6	11.6
Polyamine/Epoxy Bonding Agent	0.4*	0.4*
Ammonium Perchlorate	78.0	77.6-76.0
Aluminum (15-μ)	10.0	10.0
Ferric Oxide	0	0.4-2.0

\* Considered as binder

Note that in formulating the catalyzed propellants,  $\text{Fe}_2\text{O}_3$  replaced oxidizer--a formulation change that results in a lowered oxidizer/fuel ratio, which in turn probably results in a lower non-catalyzed burn rate

value. The significance of this mode of catalyst addition was not considered in analyzing the burn rate data.

TABLE 2  
COMPOSITION OF CTPB PROPELLANTS  
USED FOR CORRELATION ANALYSIS

Ingredient, wt %	Controls	Catalyzed
CTPB Binder	14.0	14.0
Ammonium Perchlorate	81.0	80.0-80.9
Aluminum (5- $\mu$ )	5.0	5.0
Ferric Oxide	0	0.1-1.0

Oxidizer particle size distributions used in the propellants were bimodal and trimodal blends selected from the following sizes to provide a range of AP specific surfaces:

Nominal Diameter, $\mu$	Nominal Specific Surface, $\text{cm}^2/\text{gm}$	Volume Surface Diameter, $d_{vs}$ , $\mu$
400 (As-received)	74	416
200 (As-received)	197	156
7--11 (Ground)	6,225	5.02
10 (Ground)	11,000	2.8

The HTPB propellants contained 10- $\mu$  AP along with a coarse AP fraction of either 200- $\mu$  only, 400- $\mu$  only, or a 200- $\mu$ /400- $\mu$  blend. The CTPB propellants contained 200- $\mu$  AP only, with a ground AP fraction of either 7--11  $\mu$  or 10  $\mu$ .



## FERRIC OXIDE CHARACTERISTICS

Ferric oxides used in the propellants had specific surfaces ranging from 3 to 26.4 m<sup>2</sup>/gm. These oxides had been prepared by precipitation, by calcination of yellow iron oxide, or by calcination of ferrous sulfate. Because method of preparation affects surface characteristics, such variations will appear as error in the correlations. The specific oxides used and their characteristics are given in Table 3.

TABLE 3  
CHARACTERISTICS OF FERRIC OXIDES

Method of Preparation	Density,* gm/cm <sup>3</sup>	Specific Surface,* m <sup>2</sup> /gm
Calcination of Yellow Iron Oxide	4.46	26.4
Calcination of Yellow Iron Oxide	4.95	10.0
Precipitation	4.90	9.4
Precipitation	4.90	3.7
Calcination of Ferrous Sulfate	5.15	9.2
Calcination of Ferrous Sulfate	5.18	8.4
Calcination of Ferrous Sulfate	5.15	5.1
Calcination of Ferrous Sulfate	5.18	3.9
Calcination of Ferrous Sulfate	5.15	3.0

\* Values from suppliers

## SPECIFIC PROPELLANTS

Four HTPB control formulations having AP specific surfaces of 1505, 2690, 4030, and 5257 cm<sup>2</sup>/gm and four CTPB control formulations having AP specific surfaces of 1515, 2394, 3200, and 5599 cm<sup>2</sup>/gm provided the no-catalyst burn rate data.



Rocketdyne Division  
Rockwell International

Seventeen catalyzed HTPB formulations having  $\text{Fe}_2\text{O}_3$  levels ranging from 0.4 to 2.0% and AP specific surfaces ranging from 1520 to 5395  $\text{cm}^2/\text{gm}$  and 16 catalyzed CTPB formulations having  $\text{Fe}_2\text{O}_3$  levels ranging from 0.1 to 1.0% and AP specific surfaces ranging from 1517 to 5599  $\text{cm}^2/\text{gm}$  provided the catalyzed burn rate data.

All burn rate data were from 1-pound motors fired at 77 F; a total of 295 motor firings. Motor data rather than strand data were chosen for this correlation, since the only generally reliable index of catalytic activity is performance under use conditions.



#### CORRELATION: DATA-FIT

Multiple linear regression analysis is the only dependable method for assessing the combined effects of more than one independent variable on an outcome--in this case burn rate (4). The end result of such an analysis is a "data-fit" equation containing the dependent variable and the significant independent variables in their most likely forms. Although this equation is empirical, it provides an orderly summarization of a mass of experimental data that, at first glance, may have appeared to be a chaos of meaningless numbers. To carry out such an analysis, standard computer library programs are ordinarily used.

To summarize the available burn rate data as a function of both pressure and compositional variations--AP particle size distribution and  $\text{Fe}_2\text{O}_3$  specific surface and level--reciprocal forms were used for burn rate and for all the selected independent variable inputs. Reciprocals were chosen because they have some basis in theory (5) and should, therefore, yield a reasonable "data-summary" equation.

#### CATALYST PARAMETER

The catalyst input used in the analysis and shown below approximates the ferric oxide surface area available per square centimeter of binder interface:

$$B = \left[ \frac{WS_c}{V_b} \right]^{2/5}$$

where

- $W$  -  $\text{Fe}_2\text{O}_3$  (wt %)
- $S_c$  - Specific Surface of  $\text{Fe}_2\text{O}_3$  ( $\text{cm}^2/\text{gm}$ )
- $V_b$  - Volume of Binder ( $\text{cm}^3$ )



Correlations of this parameter and burn rate when pressure and AP specific surface are fixed are given in Tables 4, 5, and 6. For these correlations, burn rate at 700 psia was selected arbitrarily.

Clearly, a host of relationships between burn rate and the catalyst parameter B are possible, particularly when the non-catalyzed case is separated from the catalyzed cases. For the correlations established here, this separation of cases was essential as reciprocal forms of dependent variables containing B would result in division by zero when no  $\text{Fe}_2\text{O}_3$  was used.

For preliminary analysis of the HTPB propellant burn rate data (6) the following reciprocal relationship was used for correlation:

$$\frac{1}{r} \sim f\left(\frac{1}{BP}\right)$$

Subsequent experience has shown that a better correlation can be obtained using the reciprocal relationship

$$\frac{1}{r} \sim f\left(\frac{1}{\ln(BP)}\right)$$

This later relationship has been used in the correlations presented herein.

#### DATA-SUMMARY EQUATIONS

Equations resulting from a multiple linear regression analysis of the burn rate, pressure and composition data from the non-catalyzed HTPB and CTPB propellants are presented below:

1. For the HTPB propellants

$$\frac{1}{r} = 3.053723 + 854.0454(1/P - 1.502416 \times 10^{-5})$$





TABLE 4  
CORRELATIONS OF CATALYST PARAMETER AND BURN RATE:  
AP SPECIFIC SURFACE  $\sim 4000 \text{ CM}^2/\text{GM}$

Formulation	AP Specific Surface, $\text{cm}^2/\text{gm}$	Catalyst Parameter B	Burn Rate, at 700 psia, in./sec	Correlation Coefficient for		Correlation Coefficient That Must be Exceeded to be Significant at 0.05 Level*
				$r = a + dB$	$r = a \exp(dB)$	
LCA-8907-1	4030	0	0.556	0.797	0.780	0.754
LCA-8904-1	3985	737.3	0.617			
LCA-8904Y-3	4010	305.76	0.576			
LCA-8905-1	3985	206.04	0.530			
LCA-8906-1	3985	343.64	0.583			
LCA-8906X-2	3985	388.14	0.600			
LCA-8904X-2	3985	464.48	0.537			

\* 1 in 20 chance that these are chance correlations

NOTE: r - burn rate

B - catalyst parameter

All other letters are constants



TABLE 5  
CORRELATIONS OF CATALYST PARAMETER AND BURN RATE:  
AP SPECIFIC SURFACE  $\sim 1520 \text{ CM}^2/\text{GM}$

Formulation	AP Specific Surface, $\text{cm}^2/\text{gm}$	Catalyst Parameter B	Burn Rate, at 700 psia, in./sec	Correlation Coefficient for		Correlation Coefficient That Must be Exceeded to be Significant at 0.05 Level
				$r - a + \text{dB}$	$r = a \exp(\text{dB})$	
LCA-8910-1	1503	0	0.271	0.951	0.946	0.754*
LCA-8909-X-2	1530	260.68	0.376			
LCA-8909-1	1530	269.995	0.391			
LCA-8908-1	1530	322.87	0.400			
LCA-8908X-2	1520	246.64	0.383			
LCA-8908Y-3	1520	370.4	0.394			
LCA-8909Y-3	1530	226.66	0.381			

\* 1 in 20 chance that these correlations are chance correlations.



TABLE 6  
CORRELATIONS OF CATALYST PARAMETER AND BURN RATE:  
AP SPECIFIC SURFACE  $\sim 1520 \text{ CM}^2/\text{GM}$

Formulation	AP Specific Surface, $\text{cm}^2/\text{gm}$	Catalyst Parameter B	Burn Rate, at 700 psia, in./sec	Correlation Coefficient for						Correlation Coefficient That Must be Exceeded to be Significant at 0.1 Level*
				$B = a + dr$	$B = a \exp(dr)$	$B = ar^d$	$B = a + d/r$	$B = \frac{1}{a + (d/r)}$	$B = \frac{r}{a + (d/r)}$	
LCA-8909X-2	1530	260.68	0.376	0.748	0.761	0.760	0.746	0.768	0.765	0.729
LCA-8909-1	1530	269.995	0.391							
LCA-8908-1	1530	322.87	0.400							
LCA-8908X-2	1520	246.64	0.385							
LCA-8908Y-5	1520	370.4	0.394							
LCA-8909Y-3	1530	226.66	0.381							

\* 1 in 10 chance that these are chance correlations



Rocketdyne Division  
Rockwell International

$$\begin{aligned}
 & -50814.2 \left( \frac{D_f}{W_f P^2} - 4.655514 \times 10^{-5} \right) \\
 & +822.9014 \left( \left[ \frac{D_f}{W_f P} \right]^2 - 3.608165 \times 10^{-4} \right) \\
 & +0.4584605 \left( \frac{D_f}{W_f P^{1/3}} - 1.794505 \right) \\
 & -1.70854 \times 10^{-5} \left( \left[ \frac{D_c}{W_c P^{1/3}} \right]^2 - 5281.061 \right) \\
 & +146279.5 \left( 1/P^2 - 2.7646 \times 10^{-6} \right)
 \end{aligned}$$

2. For the CTPB propellants

$$\begin{aligned}
 \frac{1}{r} &= 2.579005 + 1206.071 \left[ 1/P - 1.399522 \times 10^{-5} \right] \\
 & +226.9461 \left( \left[ \frac{D_f}{W_f P} \right]^2 - 7.045529 \times 10^{-4} \right) \\
 & -2176.12 \left( \frac{D_f}{W_f P^2} - 2.507215 \times 10^{-5} \right) \\
 & +1.008258 \left( \frac{D_f}{W_f P^{1/3}} - 1.66956 \right) \\
 & -0.2096639 \left( \left[ \frac{D_f}{W_f P^{1/3}} \right]^2 - 3.4761 \right) \\
 & -1.087067 \times 10^{-4} \left( \left[ \frac{D_c}{W_c P^{1/3}} \right]^2 - 1422.046 \right)
 \end{aligned}$$



$$-1.740622 \times 10^5 (1/P^2 - 2.47862 \times 10^{-6})$$

where

- r - burn rate (in./sec)
- P - pressure (psi)
- $D_f$  -  $d_{vs}$  of ground AP (microns)
- $D_c$  -  $d_{vs}$  of coarse AP or coarse AP blend (microns)
- $W_f$  - 0.01 (wt % ground AP) - weight fraction ground AP
- $W_c$  - 0.01 (wt % coarse AP or coarse AP blend) - weight fraction coarse AP

Analysis of similar data obtained from the ferric oxide-catalyzed HTPB and CTPB propellants yielded:

1. For the HTPB Propellants

$$\begin{aligned} \frac{1}{r} = & 1.886515 + 129.8563 (1/P - 1.30291 \times 10^{-3}) \\ & + 6.869025 \left( \frac{D_f}{W_f P} - 2.25281 \times 10^{-2} \right) \\ & + 52.87617 \left( \frac{1}{\ln(BP)} - 7.974412 \times 10^{-2} \right) \\ & + 74.51517 \left( \frac{D_c}{W_c P^2} - 9.797102 \times 10^{-4} \right) \\ & - 4.01712 \times 10^{-5} \left( \left[ \frac{D_c}{W_c P^{1/3}} \right]^2 - 3166.251 \right) \\ & - 0.07631436 \left( \left[ \frac{D_c}{W_c P^{1/3}} \right]^2 - 4.183392 \right) \\ & + 0.6513969 \left( \frac{D_f}{W_f P^{1/3}} - 1.782078 \right) \end{aligned}$$



2. For the CTPB Propellants,

$$\frac{1}{r} = 2.114487 + 262.6208 \left[ 1/P - 1.408446 \times 10^{-3} \right]$$

$$+ 28.3664 \left( \frac{D_f}{W_f P} - 2.052102 \times 10^{-2} \right)$$

$$- 2728.462 \left( \frac{D_f}{W_f P^2} - 4.08685 \times 10^{-5} \right)$$

$$+ 42.69885 \left( \frac{D_c}{W_c P^2} - 1.065127 \times 10^{-3} \right)$$

$$+ 25.17975 \left( \frac{1}{\ln(BP)} - 8.492485 \times 10^{-2} \right)$$

$$- 5.509124 \times 10^{-4} \left( \left[ \frac{D_c}{W_c P^{1/3}} \right]^2 - 1619.158 \right)$$

$$- 0.1771886 \left( \left[ \frac{D_f}{W_f P^{1/3}} \right]^2 - 5.144217 \right)$$

$$+ 0.2901952 \left( \frac{D_f}{W_f P^{1/3}} - 1.566285 \right)$$

$$+ 2.089561 \times 10^{-2} \left( \frac{D_c}{W_c P^{1/3}} - 58.78719 \right)$$

$$+ 5.749005 \left( \left( \frac{D_f}{W_f P^{1/3}} \right) \left( \frac{1}{\ln(BP)} \right) - 0.1347106 \right)$$



Comparison of calculated and observed burn rates along with pertinent compositional variables are presented in Appendix A. Pictorial comparisons of some of the data-fit results are also shown in Fig. 1, 2, 3, and 4. Clearly these fits are good; and from a percentage difference standpoint, they are, indeed, quite good.

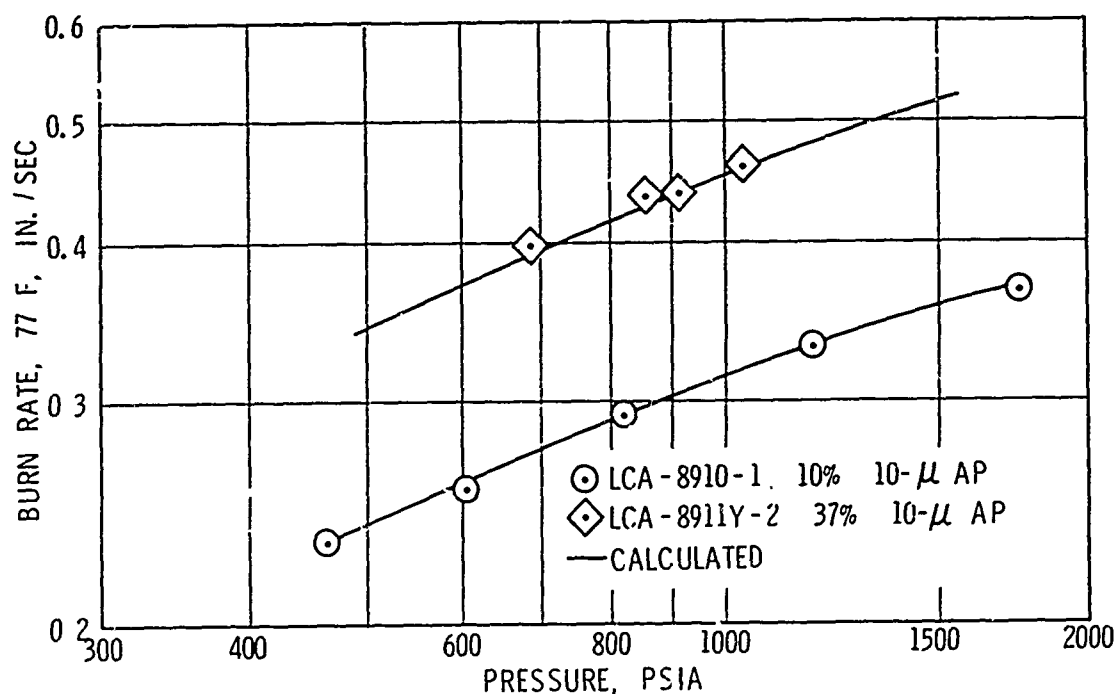


Figure 1. Comparison of Burn Rate vs Pressure Calculated from Multiple Linear Regression Analysis with Experimental Data (HTPB Propellants/No  $\text{Fe}_2\text{O}_3$ )

In the HTPB propellant cases, the greatest differences between calculated and experimental burn rates were 3.69% (no catalyst) and 12.64% ( $\text{Fe}_2\text{O}_3$  catalysis). Analysis of these same HTPB propellant data reported earlier by the principal investigator (6) did not provide nearly so good a data fit, i.e., the greatest difference between calculated and experimental burn rates were 5.67% (no catalyst) and 17.57% ( $\text{Fe}_2\text{O}_3$  catalysis).



In this earlier, less accurate analysis AP specific surface rather than a fine AP-coarse AP component breakdown was used and, as noted earlier, a direct proportionality between  $r$  and BP rather than a logarithmic proportionality between  $r$  and  $\ln(BP)$  was used when a catalyst was added to the formulation. Two standard errors of estimate about the mean  $1/r$  values of these new HTPB data fits are: for the no-catalyzed fit, 2.99%, and for the catalyst fit, 5.96%.

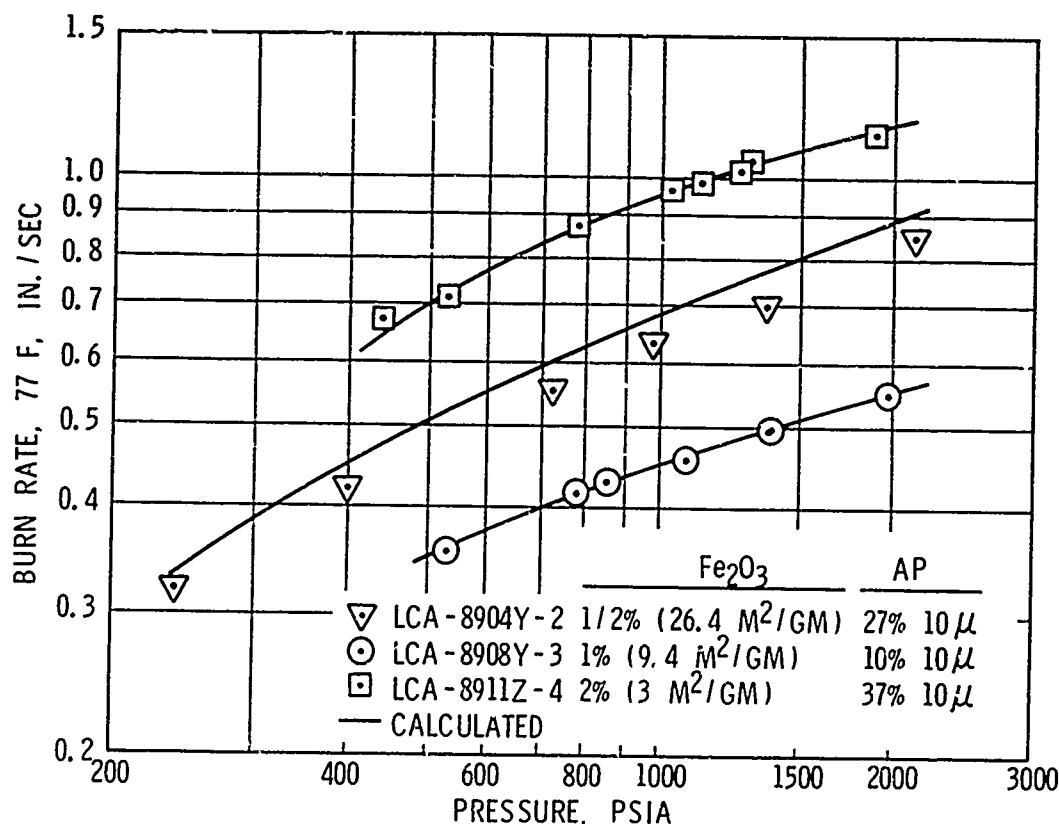


Figure 2. Comparison of Burn Rate vs Pressure Calculated from Multiple Linear Regression Analysis with Experimental Data (HTPB Propellants/Fe<sub>2</sub>O<sub>3</sub>)

In the CTPB propellant cases, the greatest differences between calculated and experimental burn rate values were 3.79% (no catalyst) and 7.98% (Fe<sub>2</sub>O<sub>3</sub> catalysis). Two standard errors of estimate about the mean  $1/r$  values of these data fits are: for the no-catalyst case, 2.74%, and for the catalyst fit, 6.66%.



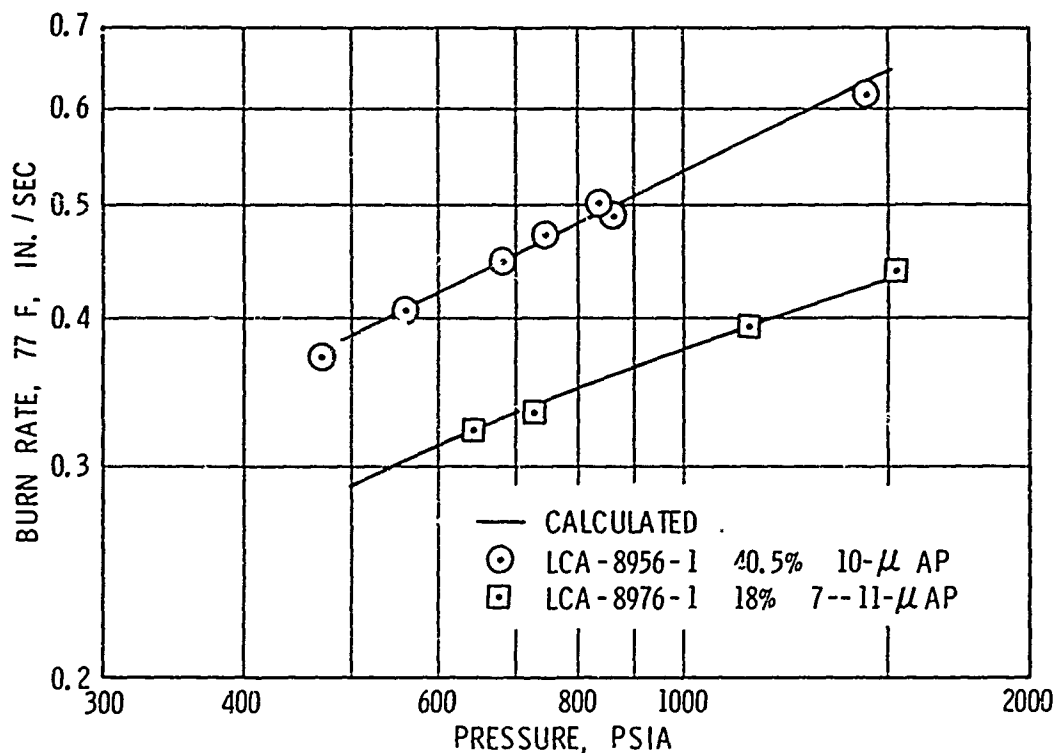


Figure 3. Comparison of Burn Rate vs Pressure Calculated from Multiple Linear Regression Analysis with Experimental Data (CTPB Propellants/No  $\text{Fe}_2\text{O}_3$ )

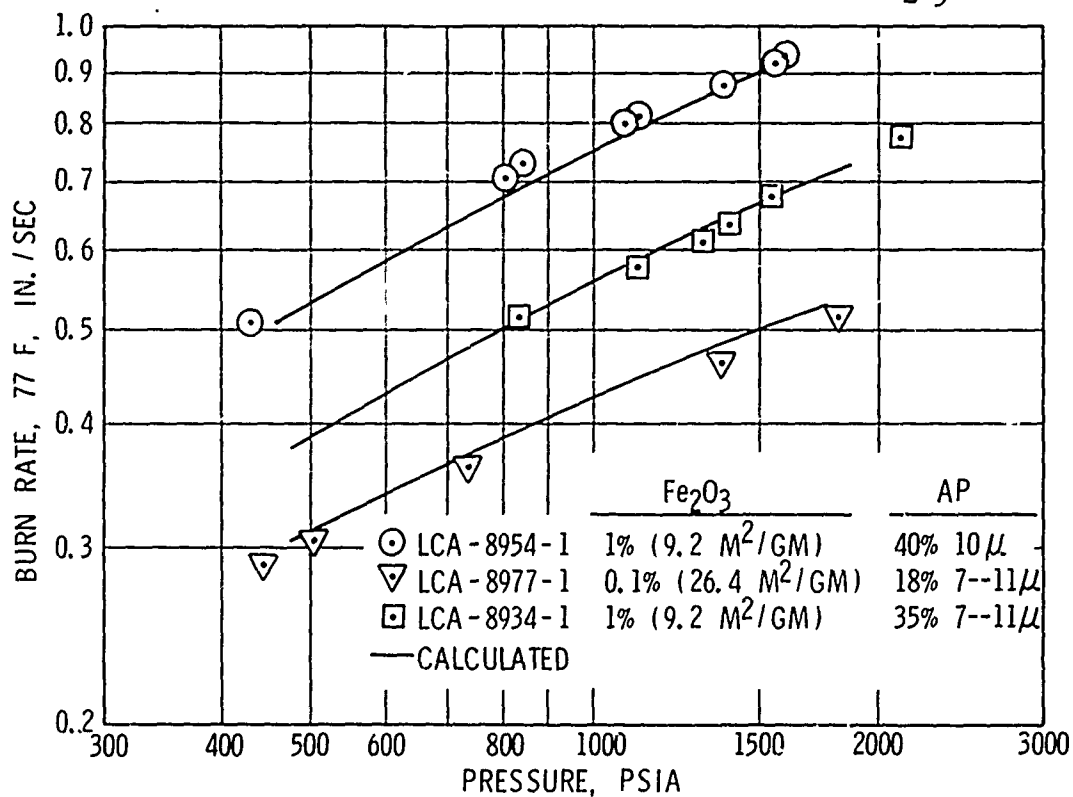


Figure 4. Comparison of Burn Rate vs Pressure Calculated from Multiple Linear Regression Analysis with Experimental Data (CTPB Propellants/ $\text{Fe}_2\text{O}_3$ )

Although these correlations are very good, there is a basic underlying weakness in them: They are based on data that are not wholly random. A consequence of this lack of randomness is discussed in a later section of this report.

#### HTPB BONDING AGENT EFFECTS

The HTPB propellants contained a polyamine epoxide bonding agent that liberates ammonia during mixing. The net results of this amine-AP reaction could be amine perchlorates at the AP-binder interface. To determine whether the presence of such perchlorates at the interface might nullify the analysis for HTPB propellants, a propellant that was identical to one of those included in the correlation except for the bonding agent was prepared and motor burn rate data were obtained at 77 F. Experimental burn rates and rates calculated from the data-summary equation for both propellants, along with the direction and magnitude of the differences between calculated and experimental rates, are shown in Table 7.

TABLE 7  
COMPARISON OF CALCULATED AND EXPERIMENTAL BURN RATES  
OF HTPB PROPELLANTS CONTAINING DIFFERENT BONDING AGENTS

Formulation	Pressure, psia	Burn Rate at 77 F, in./sec		
		Experimental	Calculated	Difference, %
LCA-8906-1	1649	0.847	0.799	- 5.67
(Contains	493	0.508	0.488	- 3.94
Polyamine/Epoxide	876	0.640	0.627	- 2.03
Bonding Agent--Used	294	0.394	0.370	- 6.09
to Obtain Data Fit	1426	0.783	0.757	- 3.32
Equation)	956	0.681	0.649	- 4.70
	607	0.550	0.537	- 2.36
LCA-8906Y-3	784	0.617	0.599	- 2.92
(Contains Acyl	1682	0.866	0.805	- 7.04
Aziridine Bonding	2446	1.061	0.921	-13.20
Agent--Not Used to	1392	0.787	0.750	- 4.70
Obtain Data Fit	1250	0.747	0.720	- 3.61
Equation)	691	0.585	0.568	- 2.91



Rocketdyne Division  
Rockwell International

Note that the calculated values for the mix with acyl aziridine bonding agent (LCA-8906Y-5) were, for all practical purposes, as good as could be expected from this data-fit equation. A good indication that bonding agent differences, which are minor from an overall composition standpoint but major from an interface composition standpoint, will not invalidate conclusions gleaned from the HTPB propellant analysis.

# CORRELATION: DISCUSSION AND CONCLUSIONS

## Fe<sub>2</sub>O<sub>3</sub> SURFACE AREA VS LEVEL

Experimental data such as those in Fig. 5, which show that Fe<sub>2</sub>O<sub>3</sub> level can be traded for Fe<sub>2</sub>O<sub>3</sub> specific surface, are the most obvious outcome expected from the data-summary equations. Hence, this outcome is presented first as Fig. 6 and 7. On these figures compositional variations that yield a burn rate of 0.5 in./sec are circled to point up the significance of a correlation analysis. In the absence of a reliable combustion model, correlations such as those obtained in the previous section provide reliable estimates of a propellant's burn rate-vs-pressure behavior, provided these estimates are interpolations.

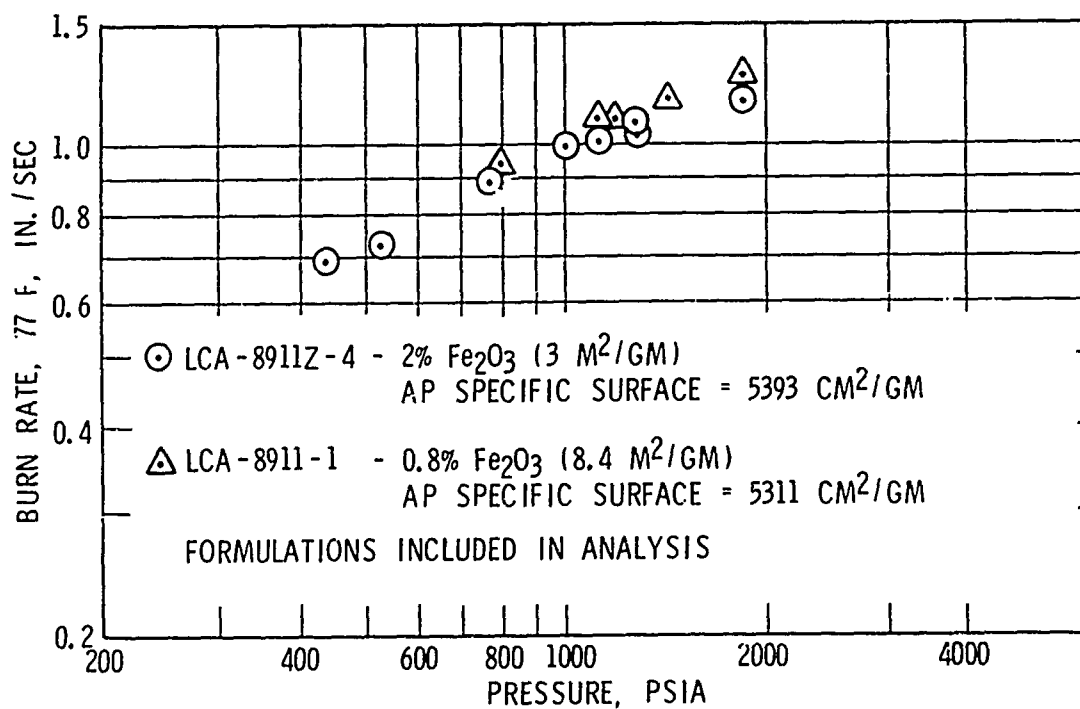


Figure 5. Effect of Low Level Fe<sub>2</sub>O<sub>3</sub> with High Specific Surface and High Level Fe<sub>2</sub>O<sub>3</sub> with Low Specific Surface

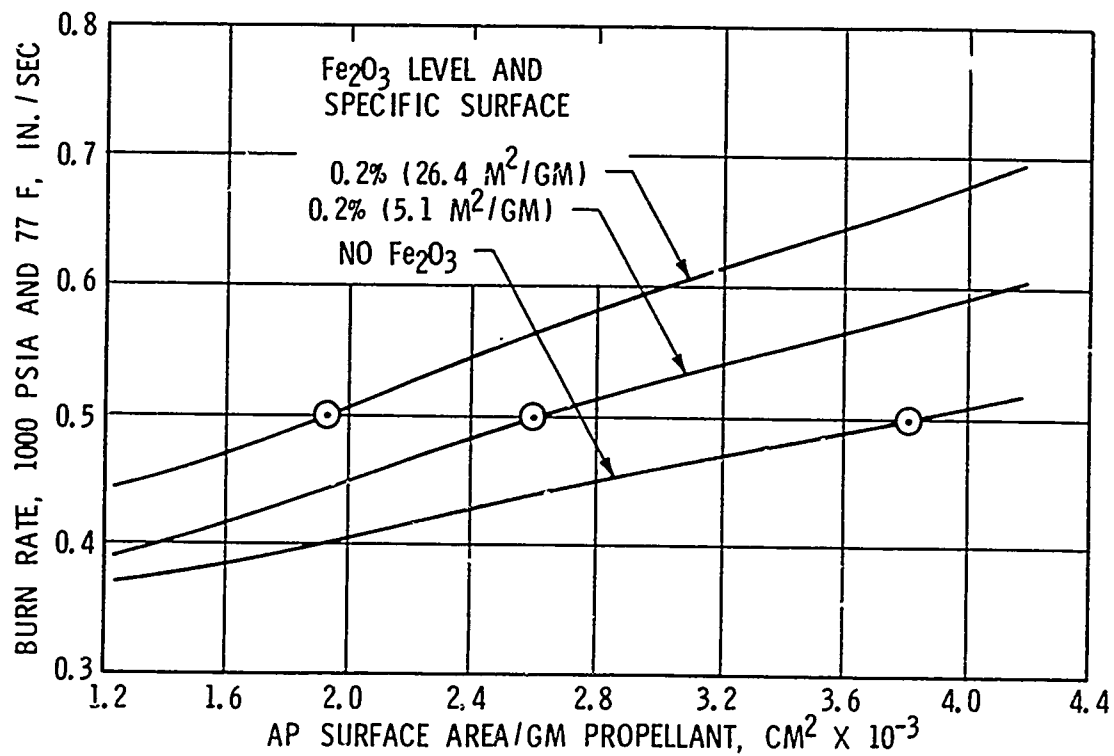


Figure 6. Burn Rates of 86% Solids CTPB Propellants Containing (1) No  $\text{Fe}_2\text{O}_3$  and (2) 0.2%  $\text{Fe}_2\text{O}_3$

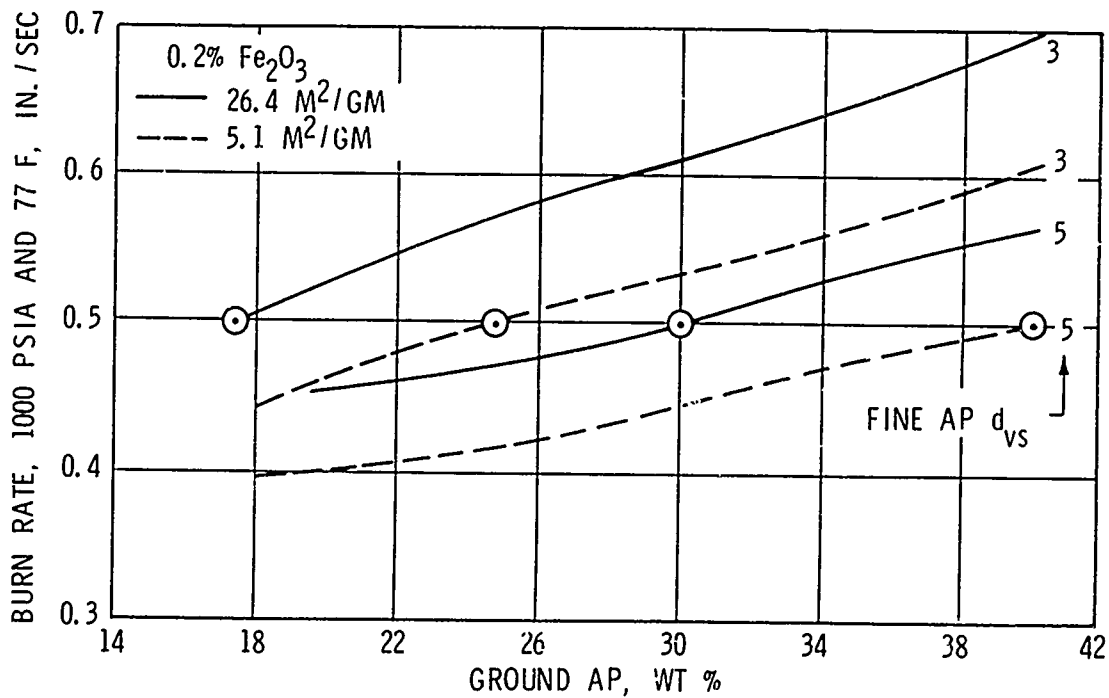


Figure 7. Burn Rates of 86% Solids CTPB Propellants Containing 0.2%  $\text{Fe}_2\text{O}_3$  as Function of Ground AP Size and Level



The well known fact that  $\text{Fe}_2\text{O}_3$  level affects burn rate will not be discussed here. However, it has not been ignored completely; i.e., the effect of  $\text{Fe}_2\text{O}_3$  specific surface is depicted at  $\text{Fe}_2\text{O}_3$  levels of 0.2 and 1.0%.

#### COARSE AP EFFECTS IN HTPB PROPELLANT

The equations representing the behavior of the HTPB propellants presented in the previous section of this report, as noted earlier in the discussion, provide a more accurate description of the behavior of these propellants than those presented earlier by the author (6). However, these more accurate equations can yield misleading outcomes. If coarse AP fraction sizes are substituted, by rote, into these expressions the outcomes in Fig. 8 and 9 can be obtained. The increase in burn rate obtained on substituting 400- $\mu$  AP for 200- $\mu$  AP when no catalyst is used can probably be disregarded since it is so small; but even so, the result is unexpected. The increase cannot, however, be ignored when a catalyst is used; it is much too large.

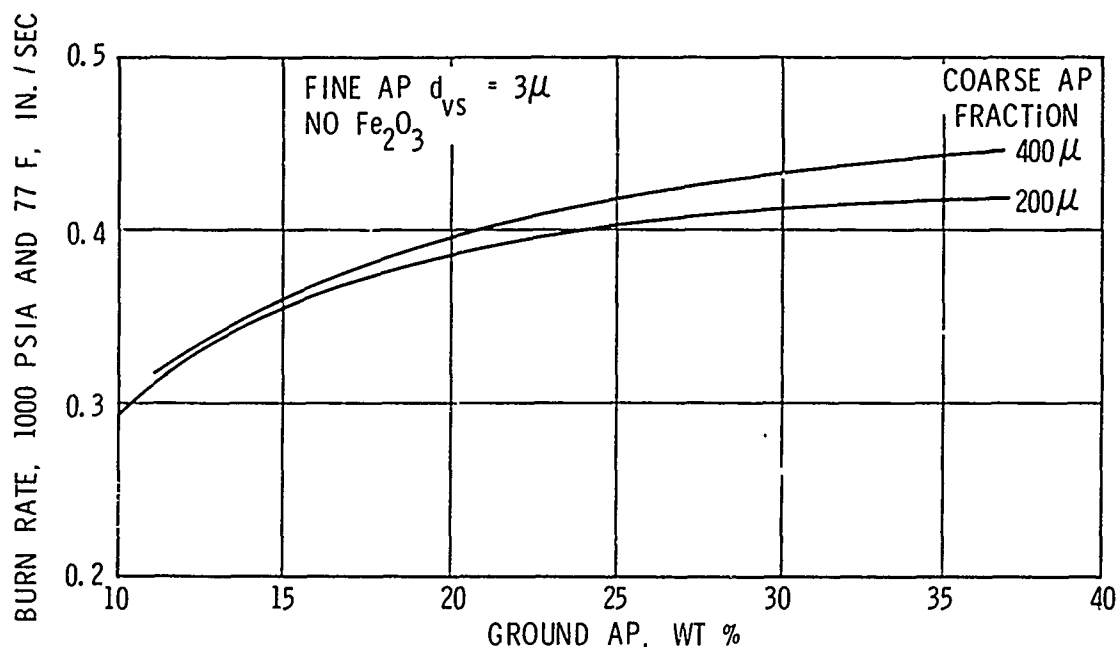


Figure 8. Burn Rates of 88% Solids HTPB Propellants Containing No  $\text{Fe}_2\text{O}_3$  Obtained by By-Rote Substitution in Data-Summary Equations

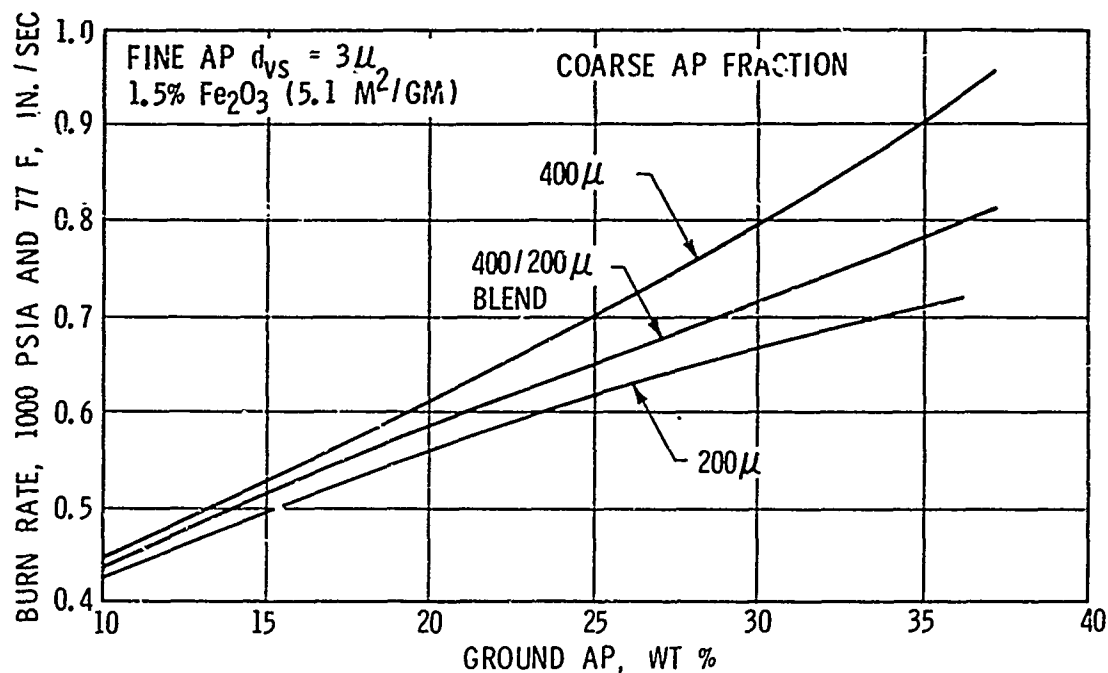


Figure 9. Burn Rates of 88% Solids HTPB Propellants Containing  $Fe_2O_3$  Obtained by By-Rate Substitution in Data-Summary Equations

The unusual response to coarse AP size inputs does not stem from error, as can be seen from the residuals-vs-coarse AP size analysis for the catalyzed propellants given in Table 8.

TABLE 8  
RESIDUALS AS FUNCTION OF COARSE AP FRACTION

AP Coarse Fraction Size, $\mu$	Number of Residuals that are		
	Positive	Zero	Negative
400	12(1)	0(0)	10(21)
400/200	17(15)	5(5)	23(25)
200	30(44)	1(0)	30(17)

Values in parenthesis are from analysis in Ref. 6, which contained bias. Other values are from  $\Delta r$ 's in Table A-5.



Because the residuals appear to be uniformly distributed regardless of coarse AP size, one must look elsewhere to account for the calculated outcomes in Fig. 8 and 9.

These outcomes arise because the coarse AP fractions used at the several fine AP levels follow a pattern that is not part of the data-summary equations (Ref. Fig. 10). To use these equations, the coarse size pattern in Fig. 10 must be followed. For example, if the ground AP level is set at 35%, a 400- $\mu$ /200- $\mu$  AP blend of  $d_{vs} = 362 \mu$  should be used to estimate burn rate.

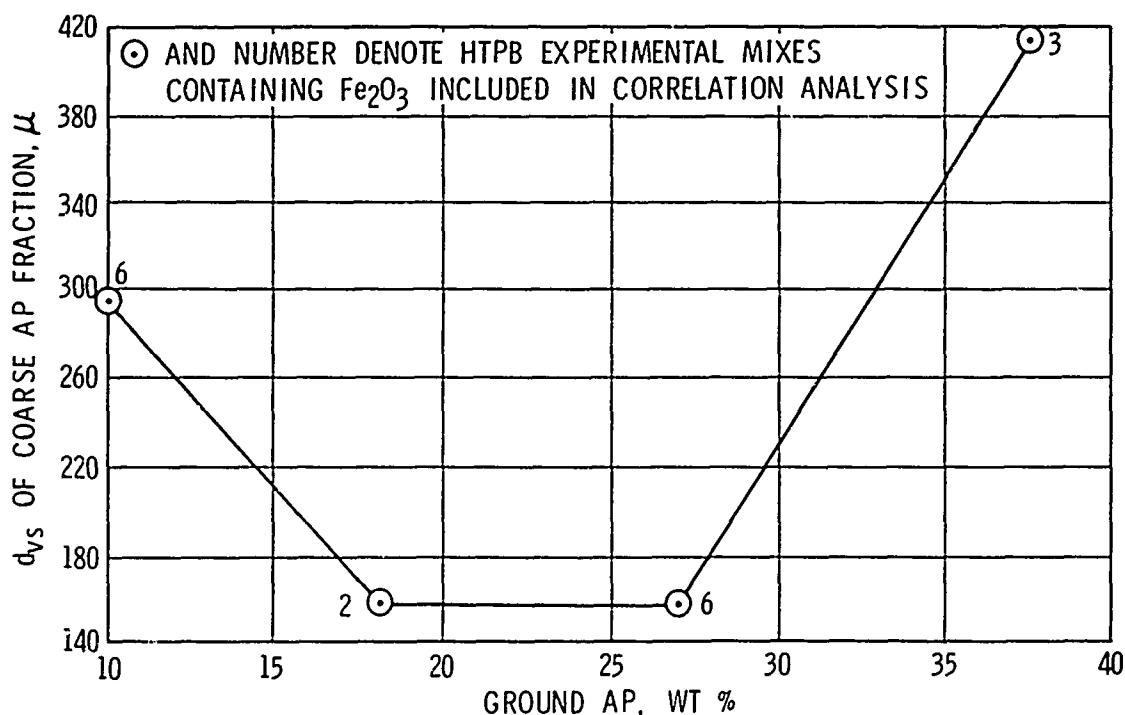


Figure 10. Pattern of Coarse AP Fraction Sizes Used in Obtaining Experimental Data that must be Adhered to in Using Data-Summary Equations for HTPB Propellants





When using this coarse AP pattern as input, the burn rate-vs-AP surface per gram of propellant data plotted in Fig. 11 are obtained. Note the unexpected upward movement in burn rate when high levels of 10- $\mu$  AP are used in conjunction with very coarse AP and ferric oxide catalysts (extreme right portion of curve).

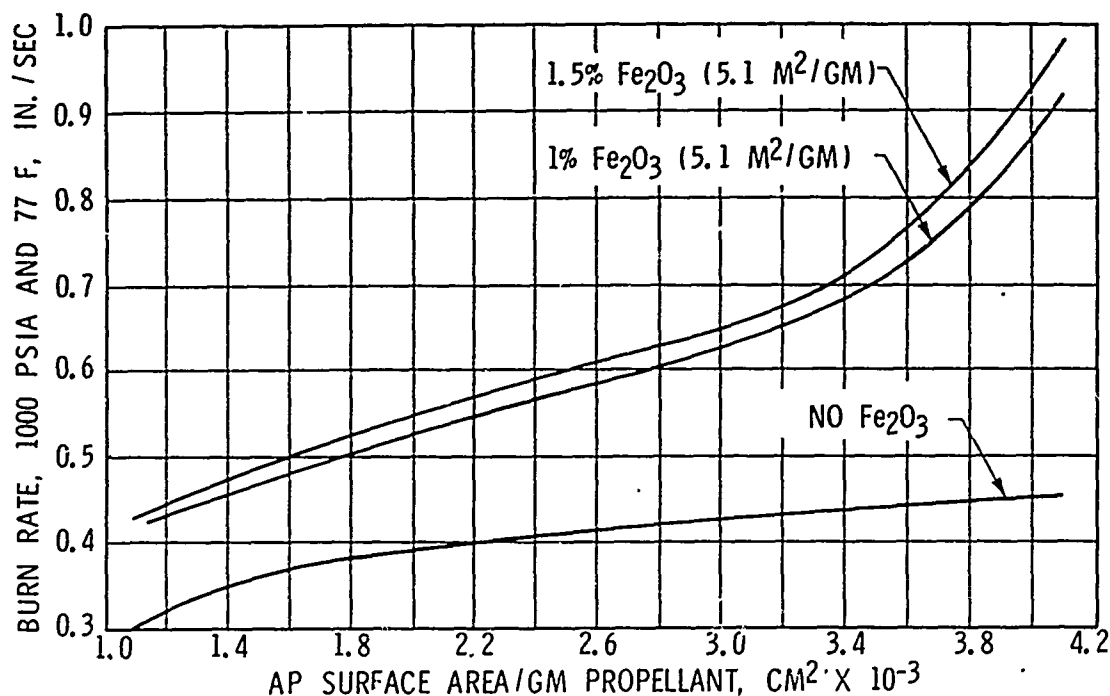


Figure 11. Burn Rates of 88% Solids HTPB Propellants With and Without  $\text{Fe}_2\text{O}_3$  Obtained Using Coarse AP Size From Fig. 10 as Inputs to Data-Summary Equations

To demonstrate that this upward movement in burn rate should actually have been expected, a propellant mix containing 35% of a different 10- $\mu$  AP grind, along with a 400- $\mu$ /200- $\mu$  AP blend,  $d_{vs} = 362 \mu$ , and 1%  $5.1 \text{ m}^2/\text{gm}$   $\text{Fe}_2\text{O}_3$  burn rate catalyst was prepared. This formulation (Table 9) is unlike any propellant included in the correlation analysis.



TABLE 9  
COMPOSITION OF BURN RATE PATTERN  
VERIFICATION MIX

	Wt %
HTPB Binder	12.00
Al (15 $\mu$ )	10.00
AP (400 $\mu$ )	58.22
AP (200 $\mu$ )	5.78
AP (10 $\mu$ )	35.00
Fe <sub>2</sub> O <sub>3</sub> (5.1 m <sup>2</sup> /gm)	1.00
	100.00

One pound motors cast from this verification mix yielded the burn rate data that are compared with the "unexpected-expected" behavior in Fig. 12. Note that the experimental burn rates compare favorably with expectation and that generally these rates are higher than calculated.

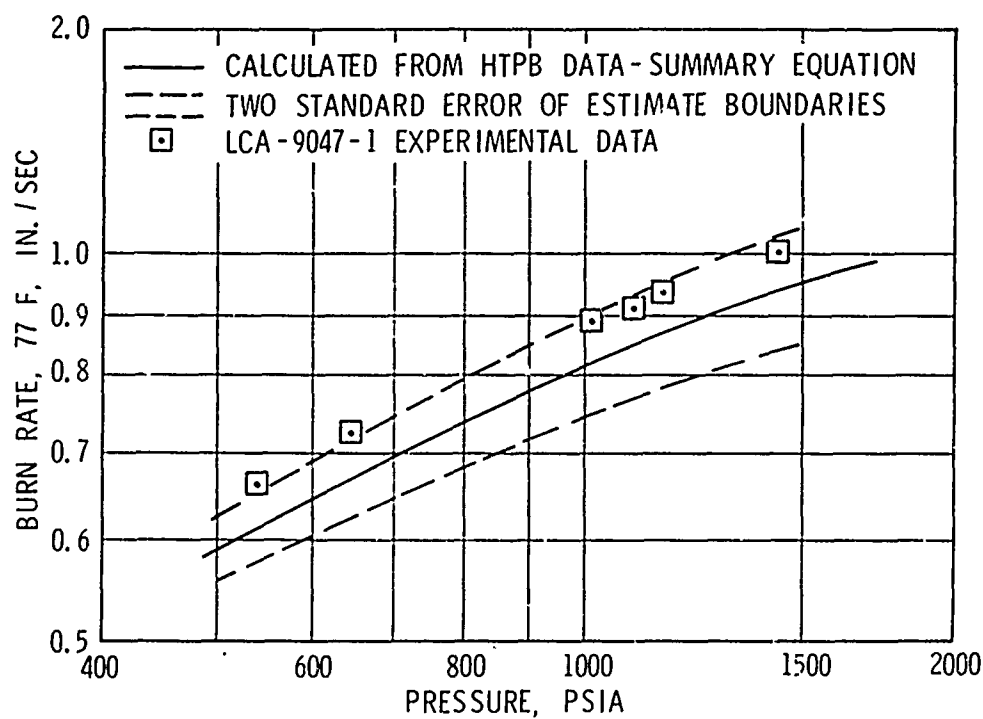


Figure 12. Comparison of Expected Burn Rate vs Pressure for LCA-9047-1 with Experimental Burn Rates



The upward thrust in the  $r$ -vs-AP surface per gram of propellant curve (Fig. 11) is apparently real. Though real, this effect of particle spacing is still a puzzlement. In further discussions of  $\text{Fe}_2\text{O}_3$  behavior in HTPB propellants only the near linear region in Fig. 11 has been considered.

#### EFFECTS OF $\text{Fe}_2\text{O}_3$ SPECIFIC SURFACE AND FINE AP LEVEL

Figures 12, 13, and 14 show there is a distinct leveling in the burn rate enhancement that can be achieved by using finer and finer  $\text{Fe}_2\text{O}_3$ . This leveling tendency sets in more slowly as the level of finely ground AP is increased.

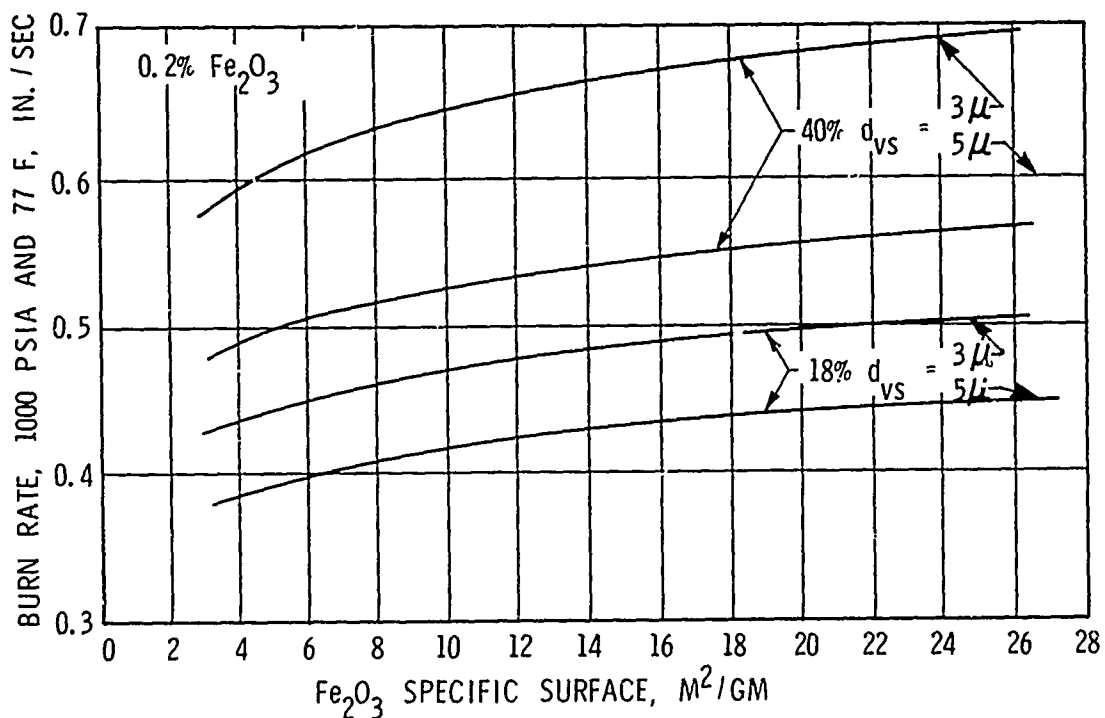


Figure 13. Effect of Ground AP Size and Level and  $\text{Fe}_2\text{O}_3$  Specific Surface on Burn Rate of 86% Solids CTPB Propellant

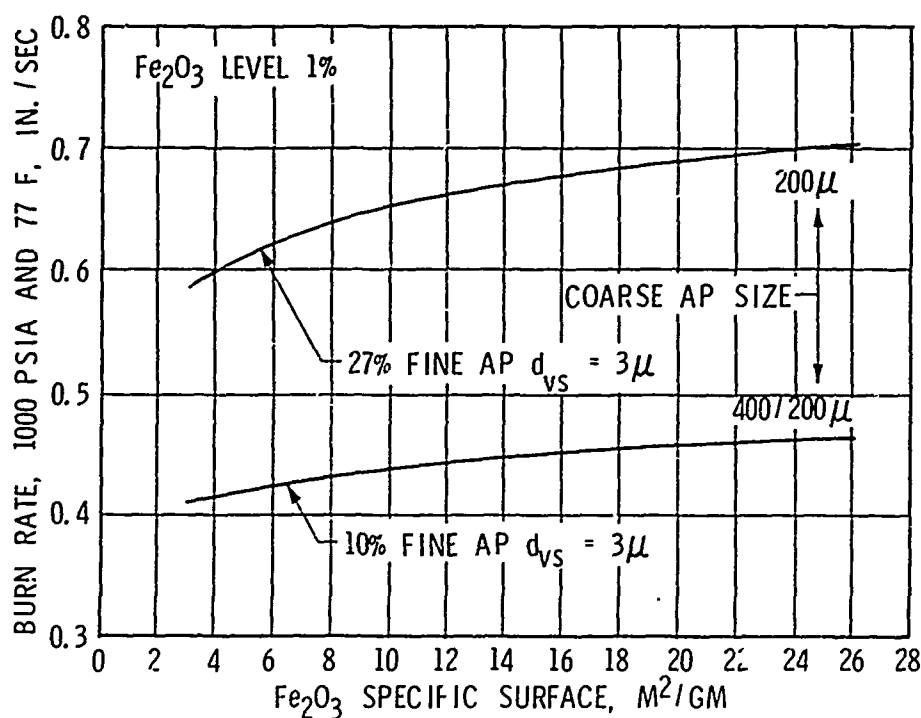


Figure 14. Effect of Ground AP Level and Fe<sub>2</sub>O<sub>3</sub> Specific Surface on Burn Rate of 88% Solids HTPB Propellants

The ratio of burn rates, catalyzed/non-catalyzed, provides a measure of effectiveness of Fe<sub>2</sub>O<sub>3</sub>. This effectiveness is plotted against Fe<sub>2</sub>O<sub>3</sub> specific surface in Fig. 15 and 16 and against AP surface per gram of propellant as Fe<sub>2</sub>O<sub>3</sub> specific surface contours in Fig. 17. Note that a given Fe<sub>2</sub>O<sub>3</sub> at a given weight level is generally more effective at high fine AP levels than at low fine AP levels. Note also the bottoming out of the Fe<sub>2</sub>O<sub>3</sub> contours in the HTPB case depicted in Fig. 17; this phenomenon occurs at approximately 12% finely ground AP.

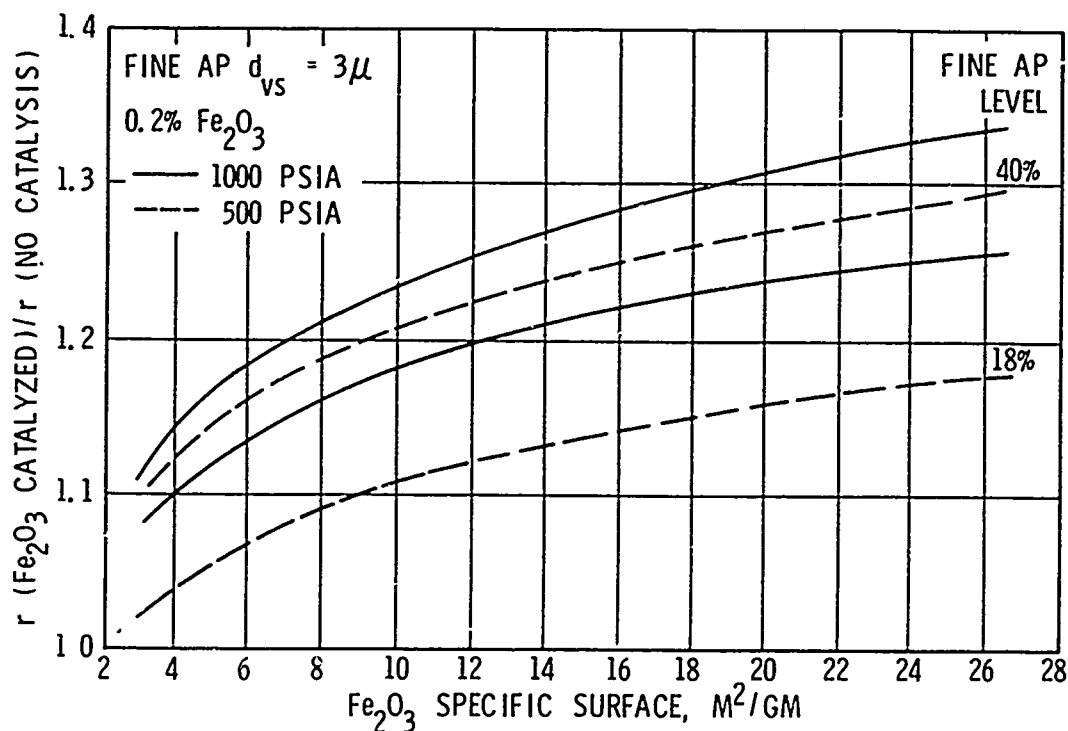


Figure 15. Effectiveness of  $\text{Fe}_2\text{O}_3$  Catalysis as Function of Fine AP Level and  $\text{Fe}_2\text{O}_3$  Specific Surface (C7PB Propellants)

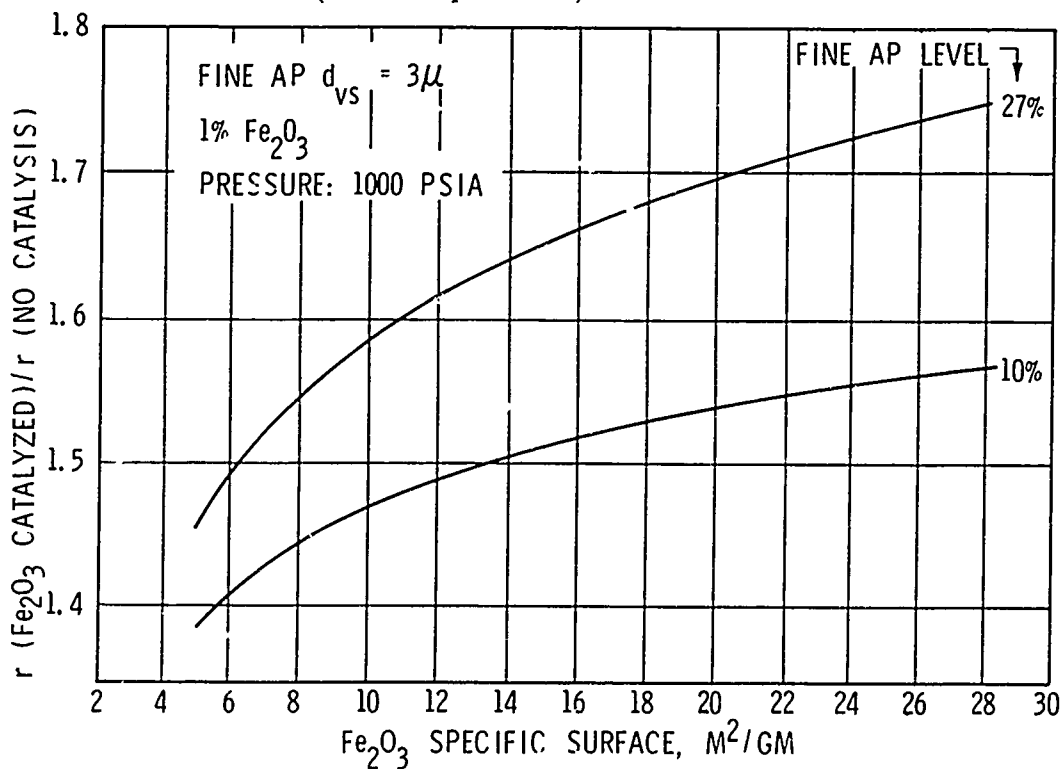


Figure 16. Effectiveness of  $\text{Fe}_2\text{O}_3$  Catalysis as Function of Fine AP Level and  $\text{Fe}_2\text{O}_3$  Specific Surface (HTPB Propellants)

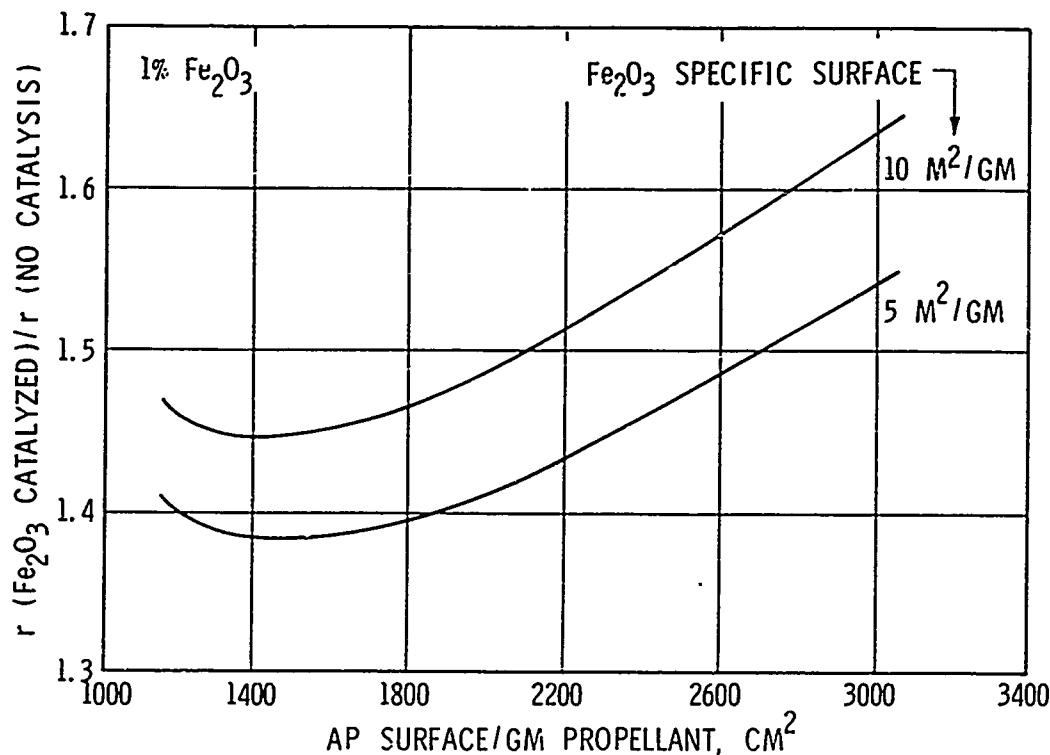


Figure 17.  $\text{Fe}_2\text{O}_3$  Specific Surface Effectiveness Contours at 1000 psia (HTPB Propellants)

Figures 18, 19, and 20 show that  $\text{Fe}_2\text{O}_3$  enhancement of burn rate is not only a function of fine AP level but also of pressure. The enhancement may be nearly constant over a wide pressure range or it may increase gradually with pressure. This latter tendency is more general than the former. Note that, in general, as the specific surface of the  $\text{Fe}_2\text{O}_3$  catalyst is increased its effectiveness is not only enhanced but also this effectiveness is more susceptible to pressure variations. These pressure dependencies probably arise because chemical reactions promoted by adsorption on heterogeneous catalyst are dependent on extent of catalytic surface and partial pressure of the reacting components. The variations in catalytic effectiveness with pressure are reflected by burn rate and pressure exponent, as shown by the data in Table 10. These effects of  $\text{Fe}_2\text{O}_3$  catalysis are also depicted in Fig. 21, 22, and 23. Generally, and collectively, effects show that an increase in burn rate is coupled with an increase in pressure exponent.

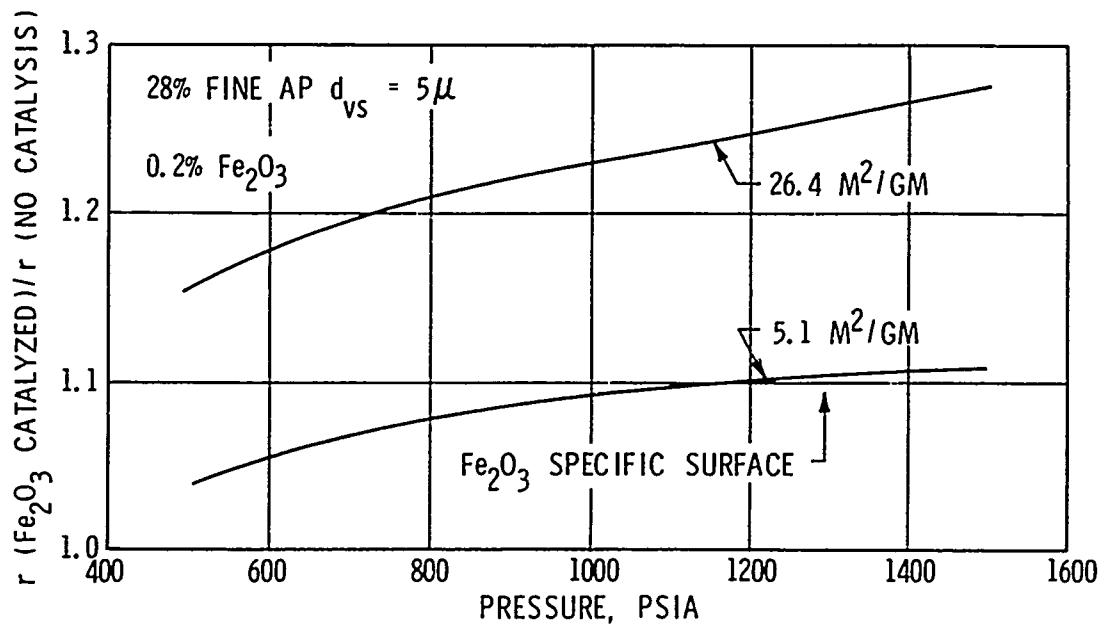


Figure 18.  $Fe_2O_3$  Effectiveness as Function of Pressure  
(CTPB Propellants)

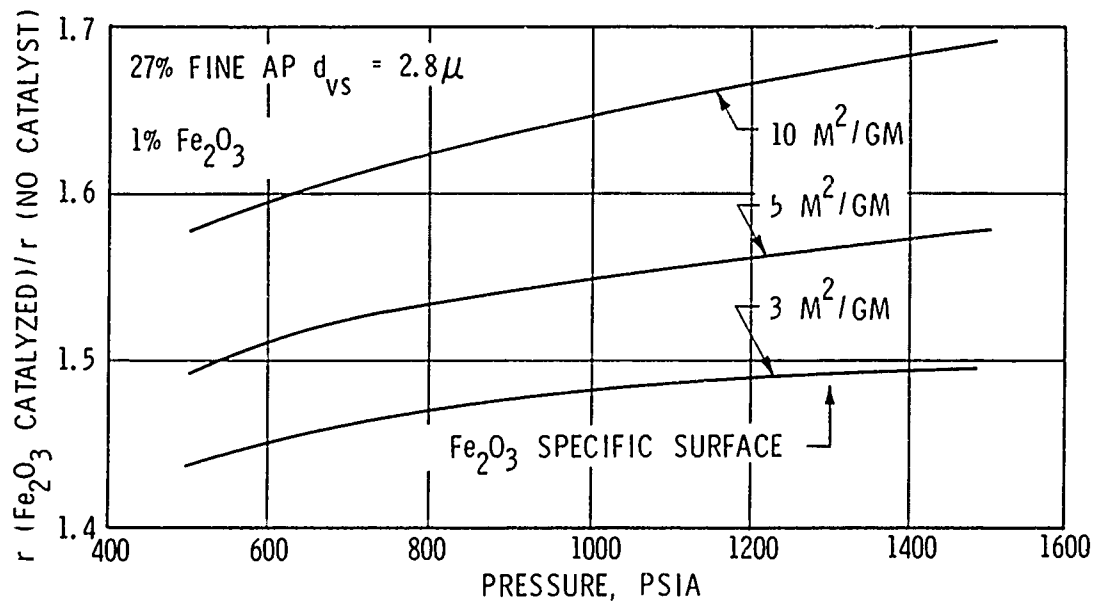


Figure 19.  $Fe_2O_3$  Effectiveness as Function of Pressure  
(HTPB Propellants)

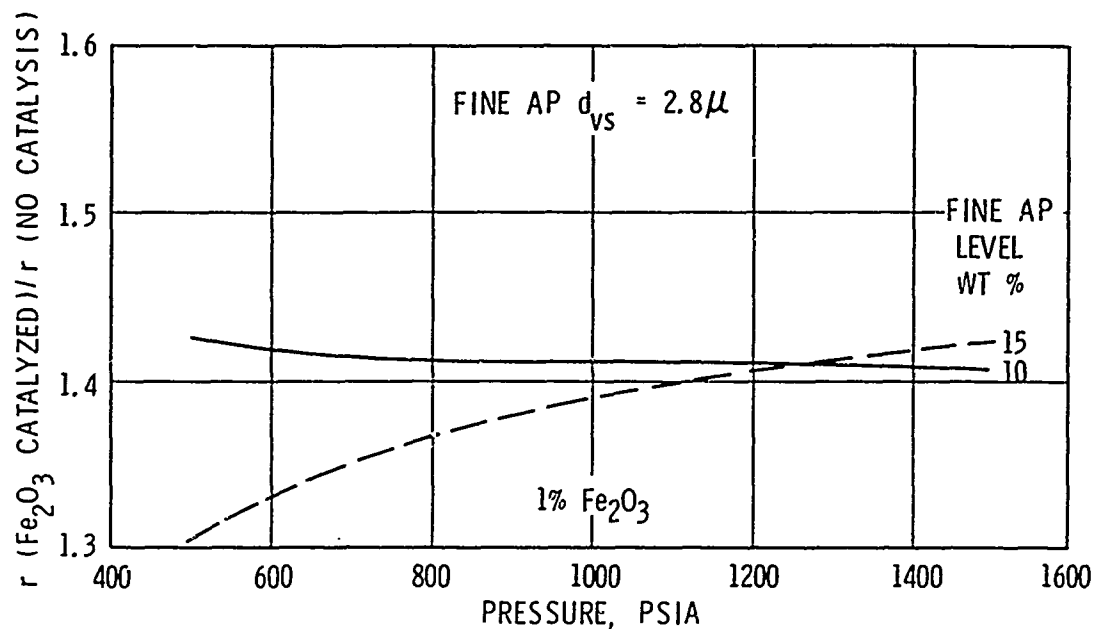


Figure 20.  $\text{Fe}_2\text{O}_3$  Effectiveness as Function of Pressure  
(ITPB Propellants)

TABLE 10  
FERRIC OXIDE SURFACE AREA EFFECT ON  
BURN RATE AND PRESSURE EXPONENT

$\text{Fe}_2\text{O}_3$ Level*	$\text{Fe}_2\text{O}_3$ Specific Surface, $\text{m}^2/\text{gm}$	Burn Rate at 1000 psia and 77 F, in./sec	Pressure Exponent (n)
0	0	0.405	0.561
1	5.9	0.611	0.598
1	8.4	0.686	0.440
1	26.4	0.751	0.475

\* ITPB Propellant: 88% Solids;  $\text{Fe}_2\text{O}_3$  replaced coarse AP



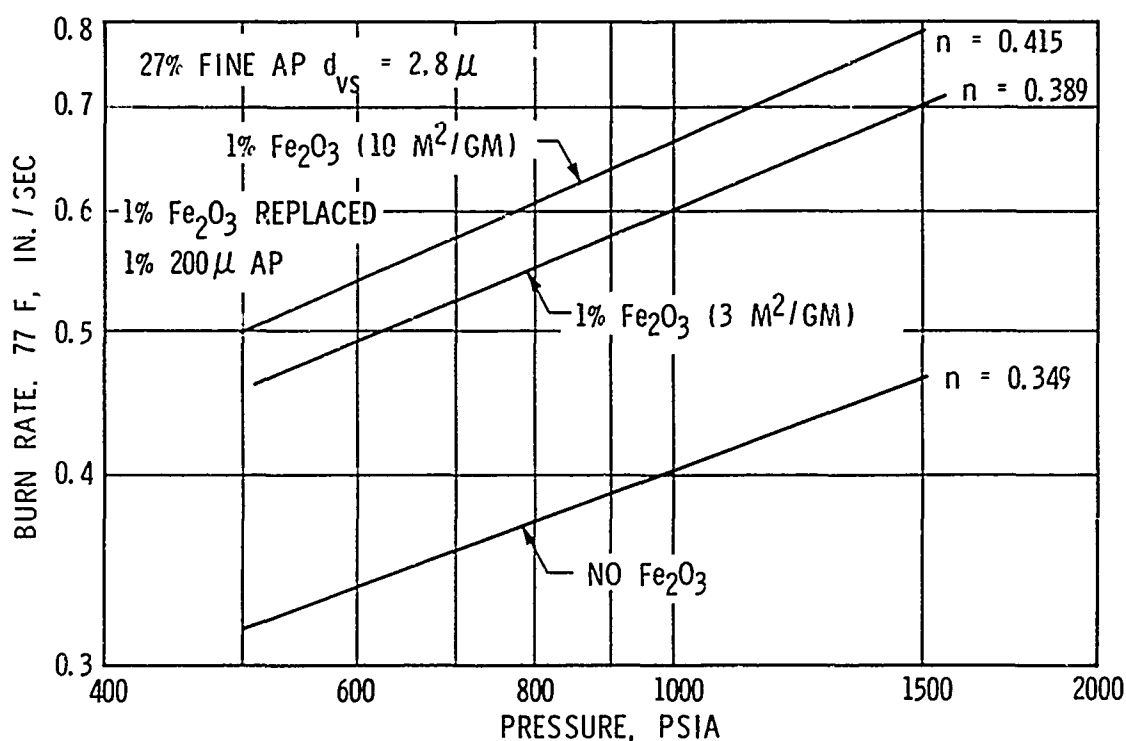


Figure 21. Effect of  $Fe_2O_3$  Specific Surface on Burn Rate and Pressure Exponent (HTPB Propellants)

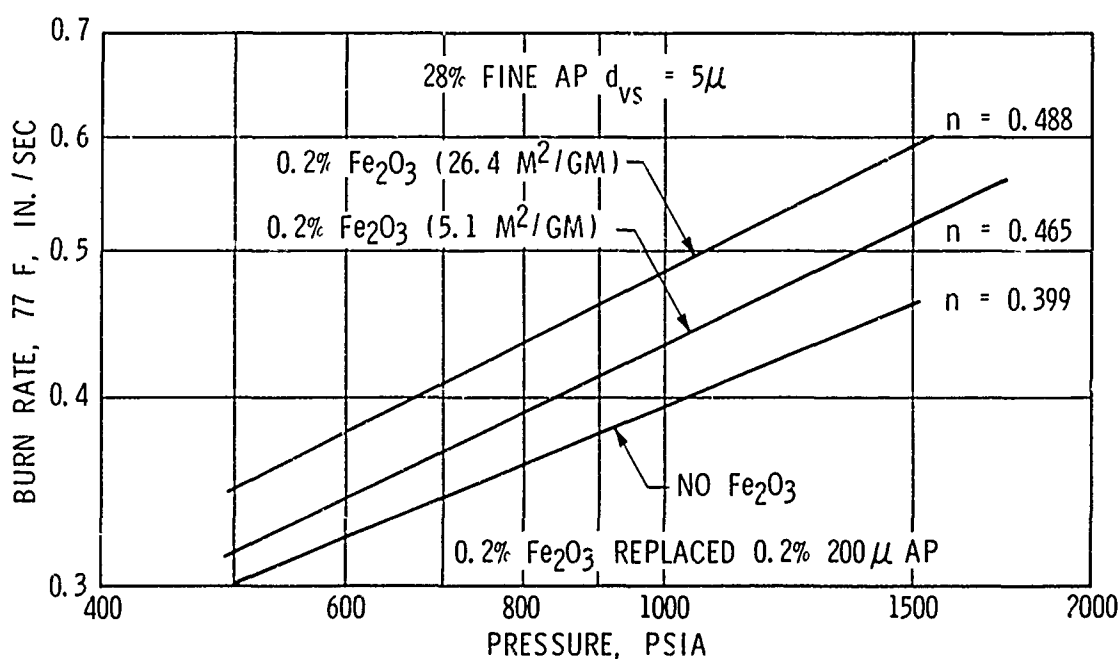


Figure 22. Effect of  $Fe_2O_3$  Specific Surface on Burn Rate and Pressure Exponent (CTPB Propellants)

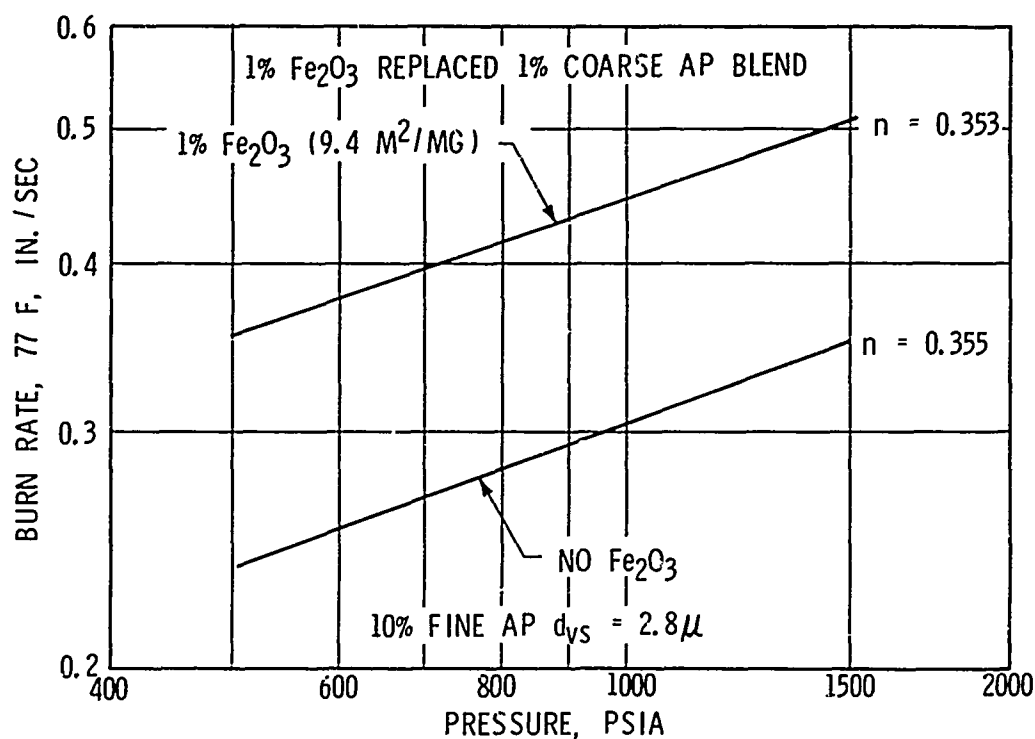


Figure 23. Effect of  $\text{Fe}_2\text{O}_3$  on Burn Rate and Pressure Exponent

This correlation effort has not proven categorically that an  $\text{Fe}_2\text{O}_3$  surface is involved in catalysis; it has however, demonstrated an association between the specific surface of the  $\text{Fe}_2\text{O}_3$  incorporated in a propellant and its effectiveness as a burn rate catalyst. Although the association is valid only over the range of the independent variable inputs, it does provide the quantitative behavior patterns needed for deriving kinetic parameters to describe the role of  $\text{Fe}_2\text{O}_3$  catalysts in propellant burning.



## QUALITATIVE CONSIDERATIONS FOR COMBUSTION MODELLING

The strong association between  $\text{Fe}_2\text{O}_3$  specific surface and catalytic effectiveness indicates that one of the kinetic models used to describe heterogeneous catalysis of chemical reactions may also describe the experimental data. AP-binder sandwich studies (3) have shown that ferric oxides play their catalytic role at the AP-binder interface. In the competing-flame combustion model, this is the primary flame where diffusion followed by chemical reaction takes place. Thus, any new kinetic expression should be inserted here.

Reaction rate equations ordinarily used to describe experimental data generally fall into two classes (7):

### 1. Homogeneous Description

$$v = k P_1^a P_2^b$$

### 2. Heterogeneous Description

$$v = \frac{k K_1 P_1 P_2}{(1 + K_1 P_1 + K_2 P_2)} \quad (\text{one example})$$

where:

v - Reaction rate

P - Partial pressure of reactants

a and b - Reaction order constants

K - Adsorption constants for active catalytic sites

k - Rate constant



A power function equation is currently used to describe reactions in the primary flame. Although catalyzed reactions can be described in this manner, equations like No. 2 above are preferred when heterogeneous catalysis is involved. In either case, the constants in these equations are considered empirical constants that can be obtained by repeated trial fits to the experimental data.

In the case of heterogeneous catalysis, several kinetic models are available for describing the reaction. Choice of model depends on probable mechanism and choice of mechanism depends on the reaction rate-vs-pressure behavior pattern. The end result of this mechanical choice process is a kinetic model most likely to mate mathematics and experimental data.

If it is assumed that the chemical processes in the AP-binder interfacial flame are second order, there are several likely kinetic expressions depending on probable mechanism from which to choose. These expressions are as follows (7):

1. Reaction between two adsorbed molecules  
(Langmuir-Hinshelwood Mechanism)

$$v = \frac{k K_1 K_2 P_1 P_2}{(1 + K_1 P_1 + K_2 P_2)^2}$$

2. Reaction between two molecules adsorbed on two different surface sites (no mutual displacement)

$$v = \frac{k K_1 K_2 P_1 P_2}{(1 + K_1 P_1)(1 + K_2 P_2)}$$

3. Reaction between a gas molecule and an adsorbed molecule  
(Langmuir-Rideal Mechanism)

$$v = \frac{k K_1 P_1 P_2}{1 + K_1 P_1 + K_2 P_2}$$

If the following arbitrary values are used in the expressions, the log-log plots in Fig. 24 are the results:

$$P_1 = P_2 = \text{Total Pressure}/2$$

$$k = 1$$

$$K_1 = 0.5$$

$$K_2 = 0.4$$

Figure 25 is a similar log-log plot of a power function expression such as is now used in the competing-flame model. Note that the power function expression and the gas molecule reacting with an adsorbed molecule mechanism both yield reaction rate-vs-pressure behavior patterns resembling propellant burn rate-vs-pressure patterns.

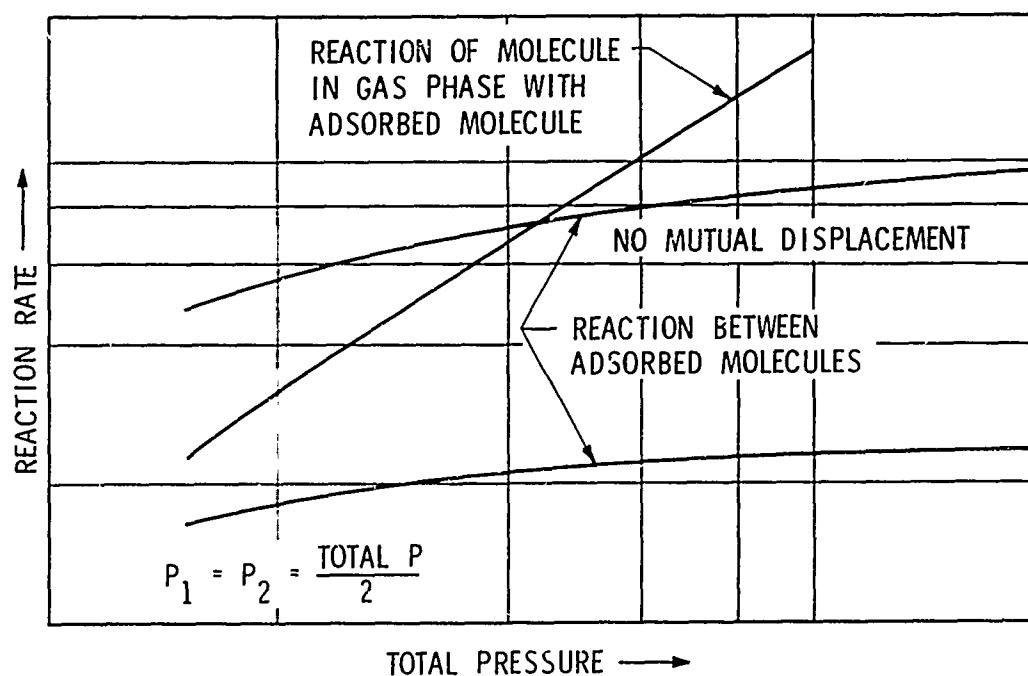


Figure 24. Reaction Patterns of Bimolecular Reaction Catalyzed by Solid Surfaces

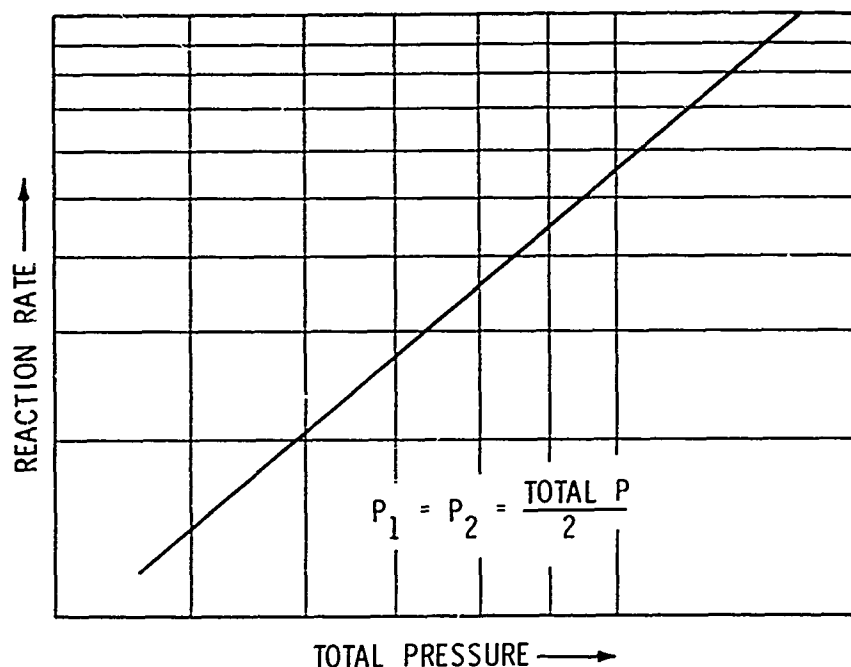


Figure 25. Reaction Pattern of Bimolecular Gas Phase Reaction

These qualitative considerations indicate that either the power function expression with some modification or a Langmuir-Rideal Mechanism should provide a reasonable kinetic expression for inserting  $\text{Fe}_2\text{O}_3$  catalysis into the multiple-flame combustion model. The latter appears to have more parameters for mating the model to the experimental data. This is not necessarily the case, however. If the KP products are very small the Langmuir-Rideal mechanism becomes

$$v = k K_1 K_2 P_1 P_2$$

a power function expression where the rate constant for the non-catalyzed case is replaced by a product of rate constant and adsorption constants.



In this power function form, the rate constant  $k$  as used now to describe kinetics in the primary flame becomes a product of a new rate constant and two adsorption coefficients. From these calculations an apparent increase in rate constant emerges when  $\text{Fe}_2\text{O}_3$  is used as catalyst. And this increase in rate constant should be reflected as an upward shift in a log-log  $r$ -vs- $P$  plot very much like the upward shifts depicted in Fig. 21, 22, and 23.

The question naturally arises: How large must the increase in primary flame reaction rate constant be in order to account for the increases in burn rate attainable from  $\text{Fe}_2\text{O}_3$  catalysis? To answer this question, the parameters listed in AFOSR-TR-74-0985 (2) were put into the multiple-flame combustion model. A primary flame rate constant of 30 (standard value) and this same rate constant increased by 2 and 3 orders of magnitude yielded the data plotted in Fig. 26. A thousand-fold increase in rate constant yielded only a modest increase in burn rate. This increase in rate is not nearly as large as can be obtained by  $\text{Fe}_2\text{O}_3$  catalysis--Ref, for example, Fig. 23.

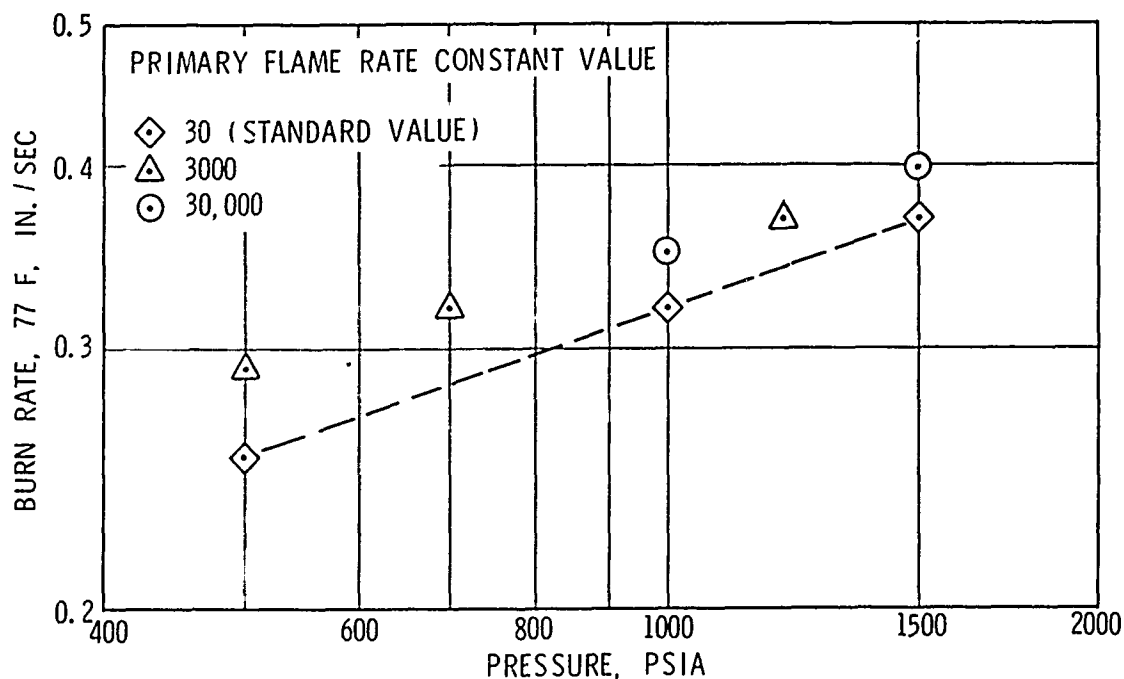


Figure 26. Burn Rates Calculated from Multiple-Flame Combustion Model Using Parameter Inputs from Ref. 2 with Primary Flame Rate Constants Varied



This much upward shift in the log-log r-vs-P plot in Fig. 26 can be effected by only a small change in the average flame height factor (the "adjustment" factor used to position the flame nearer or farther from the burning surface so combustion model predictions match experimental outcomes). Figure 27 shows the effect of a decrease in this factor from the standard value, 0.5, to 0.3, a value that moves the flame front nearer the burning surface.

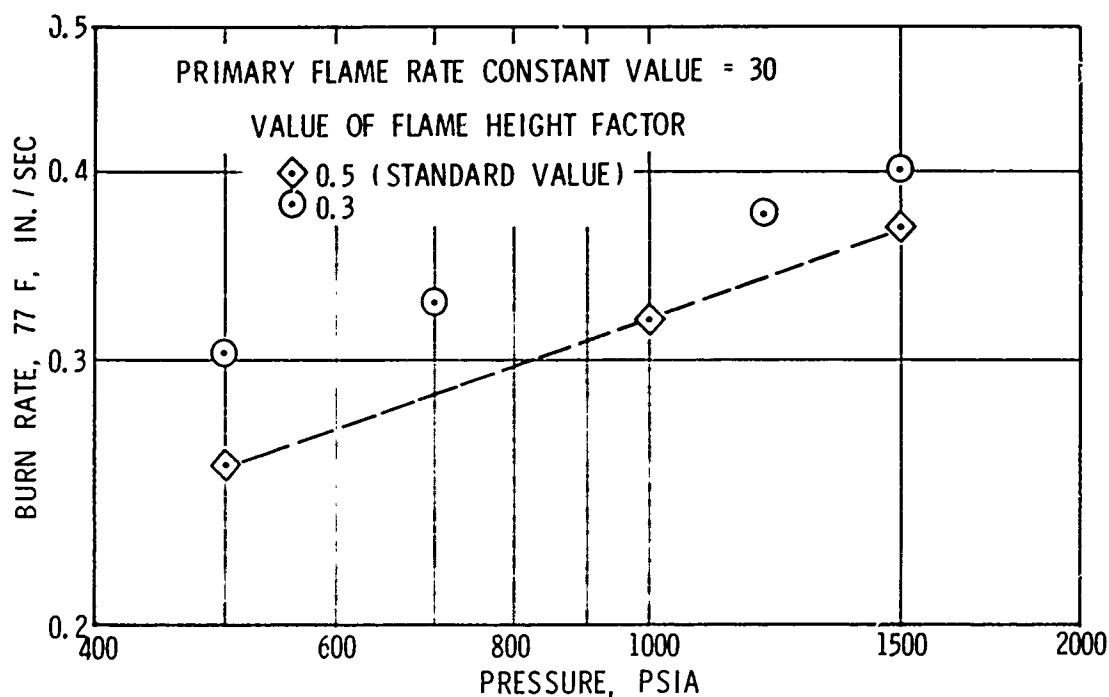


Figure 27. Burn Rates Calculated from Multiple-Flame Combustion Model Using Parameter Inputs from Ref. 2 with Average Flame Height Factors Varied

Apparently, increases in burn rate large enough to account for  $\text{Fe}_2\text{O}_3$  catalysis by a several-fold increase in the primary flame reaction rate constant cannot be obtained from the multiple-flame combustion model. Therefore, some restructuring of the model will be required.





## FINAL STATUS AND RECOMMENDATIONS FOR FURTHER STUDY

Correlation analyses of burn rate data obtained from 88% solids loaded HTPB propellants and 86% solids loaded CTPB propellants have yielded quantitative relationships between  $\text{Fe}_2\text{O}_3$  level and specific surface and AP particle size distributions. Within the bounds of the independent variable inputs used to deduce these relationships, interpolated results are within  $\pm 15\%$  of experimental results. And from these relationships the quantitative effects of variation in  $\text{Fe}_2\text{O}_3$  specific surface at two  $\text{Fe}_2\text{O}_3$  levels have been depicted. Initial efforts to use these correlations to extend the multiple-flame combustion model to include  $\text{Fe}_2\text{O}_3$  catalysis indicate some restructuring of this model will be required. Efforts to utilize the background information generated to date should continue.

Since the work reported herein is limited to only one type of catalyst, the red iron oxides, additional experimental work coupled with a correlation analysis is needed to cover the entire spectrum of iron oxide catalysts and to obtain a similar insight into the use of copper chromite catalysis. Such effort should provide answers to the following:

1. Do other iron oxides, e.g., hydrated yellow oxides, exhibit a similar surface area catalytic effectiveness correlation? If so, when the specific surface is fixed, is the catalytic activity of the several iron oxides associated with iron content?
2. Do the copper chromites exhibit a surface area catalytic effectiveness correlation? Is their effectiveness associated more with chromium level than copper level or vice versa?

Some consideration should also be given to temperature effects. The results reported herein indicate that increasing the specific surface of  $\text{Fe}_2\text{O}_3$  at a fixed level not only results in an increased burn

rate but also in an increased pressure exponent. Is this effect of  $\text{Fe}_2\text{O}_3$  specific surface on  $n$  reflected by  $\pi_k$  or is there a compensating effect on  $\sigma_p$ ? To provide an answer to this question and to others prompted by it, experimental data must be obtained at several temperatures.

The effect of AP particle spacing encountered in the HTPB propellant case, not considered in depth in studies thus far, has also been encountered in slightly altered form at very low burn rates, as is shown in Fig. 28. Both sets of data indicate AP particle spacing plays a role in burning (Neither set stems from scientifically planned experimentation). The possibility that spacing has a significant role in burning should be evaluated experimentally. If it is significant only when formulations contain very coarse AP, the AP size distributions that lead to AP particle spacing effects should be established.

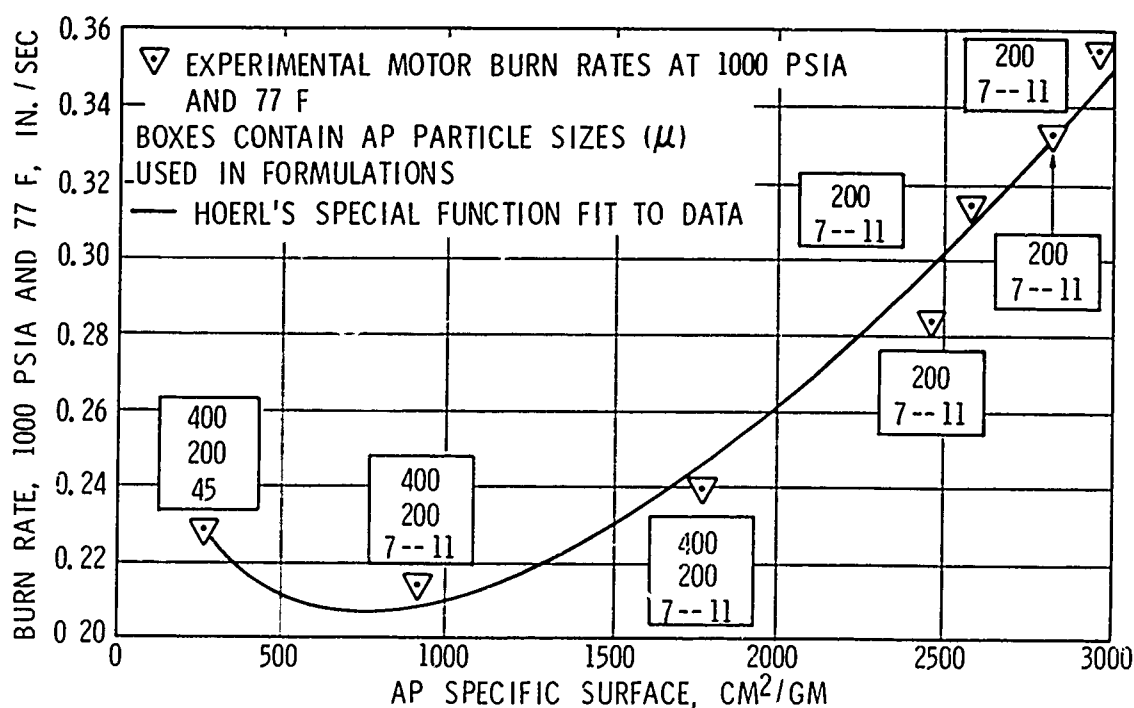


Figure 28. Effect of Particle Size Distribution on Burn Rate

Finally, the additional background on the iron oxides and the new background on the copper chromites should be used to extend the competing-flame model to the more general case of heterogeneous catalysis.



#### REFERENCES

1. Beckstead, M. W.; R. L. Derr; and C. F. Price: "A Model of Composite Solid Propellant Combustion Based on Multiple Flames," AIAA Journal, Vol. 8, No. 9, 2200 (1970).
2. Sammons, G. D.: "Multiple-Flame Combustion Model FORTRAN IV Computer Program," AFOSR-TR-74-0985, 1974.
3. Strahle, W. C.; J. C. Handley; and T. T. Milkie: "AP-HTPB Sandwich Combustion Studies," 9th JANNAF Combustion Meeting, Vol. II (September, 1972).
4. Daniel, C.; and F. S. Wood: "Fitting Equations to Data," Wiley-Interscience, (1971).
5. Summerfield, M.; et al: "Burning Mechanisms of Ammonium Perchlorate Propellants," Progress in Astronautics and Aeronautics, 1, New York: Academic Press, 1960, pp. 207-226.
6. Burnside, C. H.: "Correlation of Ferric Oxide Surface Area and Propellant Burning Rate," AIAA Paper 75-234, Presented at the AIAA 13th Aerospace Sciences Meeting, (January 1975).\*
7. Laidler, K. J.: "Chemical Kinetics," 2nd ed. McGraw-Hill Book Company, 1965.

---

\*There are four errors in this paper: In Tables A-1 and A-2, LCA-8911Y-2, LCA-8911-1, LCA-8911X-3 and LCA-8911Z-4 are listed as containing blends of 200- $\mu$  and 10- $\mu$  AP particles; this should read blends of 400- $\mu$  and 10- $\mu$  AP particles.



Rocketdyne Division  
Rockwell International

APPENDIX A

COMPARISON OF BURN RATES CALCULATED  
FROM REGRESSION ANALYSIS WITH  
THE EXPERIMENTAL VALUES

## APPENDIX A

### COMPARISON OF BURN RATES CALCULATED FROM REGRESSION ANALYSIS WITH THE EXPERIMENTAL VALUES

In the tables that follow  $\Delta r$  is defined as follows:

$$\Delta r = \frac{\text{Calculated } r - \text{Observed } r}{\text{Observed } r}$$

TABLE A-1

### COMPARISON OF CALCULATED AND EXPERIMENTAL BURN RATES OF NON-CATALYZED HTPB PROPELLANTS

(Regression Analysis Index of Determination = 0.997)

(Mean  $1/r = 5.053725$ ;  $\sigma$  (est) = 0.0454)

Formulation	Pressure, psia	Burn Rate at 77 F, in./sec		$\Delta r, \%$
		Experimental	Calculated	
LCA-8907-1	1681	0.491	0.480	-2.65
AP Specific Surface	728	0.352	0.365	+3.69
- 4030 cm <sup>2</sup> /gm	740	0.364	0.367	+0.82
Blend of 200- $\mu$ and	702	0.359	0.360	+0.27
10- $\mu$ AP Particles	641	0.346	0.348	+0.58
	427	0.302	0.297	-1.66
	404	0.296	0.291	-1.69
	343	0.271	0.274	+1.01
LCA-8910-1	345	0.208	0.205	-1.44
AP Specific Surface	376	0.209	0.212	+1.44
- 1505 cm <sup>2</sup> /gm	1175	0.328	0.324	-1.22
Blend of 400- $\mu$ , 200- $\mu$	821	0.290	0.286	-1.38
and 10- $\mu$ AP Particles	605	0.254	0.255	+0.39
	465	0.231	0.231	0.00
	1767	0.366	0.367	+0.27
	2222	0.380	0.391	+2.89
LCA-8926C-2	1108	0.387	0.390	+0.90
AP Specific Surface	844	0.360	0.359	-0.28
- 2690 cm <sup>2</sup> /gm	656	0.334	0.331	-0.90
Blend of 200- $\mu$ and	601	0.325	0.322	-0.92
10- $\mu$ AP Particles	554	0.314	0.315	+0.32
	381	0.284	0.285	+0.35
	1537	0.454	0.429	-1.15
	1706	0.447	0.440	-1.57
LCA-8911Y-2*	1034	0.459	0.458	-0.22
AP Specific Surface	910	0.432	0.438	+1.39
- 5257 cm <sup>2</sup> /gm	860	0.433	0.429	-0.92
Blend of 400- $\mu$ and	686	0.390	0.392	+0.51
10- $\mu$ AP Particles	686	0.395	0.392	-0.76

\* Some instability encountered at high pressures--above 1034 psia



TABLE A-2  
COMPARISON OF CALCULATED AND EXPERIMENTAL BURN RATES  
OF NON-CATALYZED CTPB PROPELLANTS  
(Regression Analysis Index of Determination = 0.998)  
(Mean  $1/r = 2.579003$ ;  $\sigma$  (est) = 0.0353)

Formulation	Pressure, psia	Burn Rate at 77 F, in./sec		$\Delta r, \%$
		Experimental	Calculated	
LCA-8972-1	694	0.346	0.348	+0.58
AP Specific Surface	1236	0.438	0.440	+0.46
- 2394 cm <sup>2</sup> /gm	434	0.291	0.290	-0.34
Blend of 200- $\mu$ and 7-11- $\mu$	484	0.306	0.302	-1.31
AP Particles	805	0.365	0.370	+1.37
	1134	0.425	0.425	-0.47
	264	0.232	0.232	0.00
LCA-8966-1	438	0.322	0.323	+0.31
AP Specific Surface	724	0.388	0.393	+1.29
= 3200 cm <sup>2</sup> /gm	583	0.359	0.359	0.00
Blend of 200- $\mu$ and 7-11- $\mu$	550	0.356	0.351	-1.40
AP Particles	1507	0.548	0.539	-1.64
	1195	0.485	0.488	-0.62
	958	0.438	0.444	+1.37
	678	0.384	0.382	-0.52
LCA-8956-1	829	0.499	0.486	-2.61
AP Specific Surface	2041	0.764	0.739	-3.27
= 5599 cm <sup>2</sup> /gm	561	0.404	0.399	-1.24
Blend of 200- $\mu$ and 10- $\mu$	743	0.464	0.461	-0.65
AP Particles	680	0.445	0.443	-0.45
	1428	0.607	0.630	+3.79
	856	0.485	0.493	+1.65
	470	0.372	0.379	+1.88
LCA-8976-1	1882	0.455	0.453	-0.44
AP Specific Surface	2255	0.470	0.477	+1.49
- 1515 cm <sup>2</sup> /gm	590	0.241	0.241	0.00
Blend of 200- $\mu$ and 7-11- $\mu$	751	0.353	0.355	+0.60
AP Particles	667	0.321	0.324	+0.93
	1133	0.391	0.389	-0.51
	1525	0.437	0.426	-2.52

TABLE A-3  
COMPARISON OF CALCULATED AND EXPERIMENTAL BURN RATES  
OF  $\text{Fe}_2\text{O}_3$ -CATALYZED HTPB PROPELLANTS  
(Regression Analysis Index of Determination = 0.994)  
(Mean  $1/r = 1.886515$ ;  $\sigma$  (est) = 0.0562)

Formulation	Pressure, psia	Burn Rate at 77 F, in./sec		$\Delta r, \%$
		Experimental	Calculated	
LCA-8926X-3	1065	0.601	0.611	+1.66
1. 2% $\text{Fe}_2\text{O}_3$ ; 10 $\text{m}^2/\text{gm}$	1287	0.646	0.657	+1.70
	1736	0.742	0.734	-1.08
2. AP Specific Surface = 2756 $\text{cm}^2/\text{gm}$	538	0.463	0.460	-0.65
	621	0.492	0.490	-0.41
Blend of 200- $\mu$ and 10- $\mu$ AP Particles	958	0.581	0.586	-0.86
	1841	0.756	0.750	-0.79
	359	0.390	0.378	-3.08
LCA-8926-1	1034	0.533	0.551	-3.38
1. 2% $\text{Fe}_2\text{O}_3$ ; 3 $\text{m}^2/\text{gm}$	340	0.352	0.344	-2.27
	493	0.408	0.410	+0.49
2. AP Specific Surface = 2756 $\text{cm}^2/\text{gm}$	563	0.428	0.434	+1.40
	828	0.497	0.507	+2.01
Blend of 200- $\mu$ and 10- $\mu$ AP Particles	929	0.515	0.530	+2.91
	1374	0.588	0.611	+3.91
	1773	0.661	0.668	-1.06
LCA-8911-1	1208	1.072	1.026	-4.29
1. 0.8 % $\text{Fe}_2\text{O}_3$ ; 8.4 $\text{m}^2/\text{gm}$	819	0.922	0.886	-3.90
	2689	1.470	1.312	-10.75
2. AP Specific Surface = 5311 $\text{cm}^2/\text{gm}$	1868	1.247	1.186	-4.89
	1414	1.123	1.081	-3.74
Blend of 400- $\mu$ and 10- $\mu$ AP Particles	1177	1.053	1.017	-3.42
LCA-8911Z-4	1866	1.139	1.182	+3.78
1. 2% $\text{Fe}_2\text{O}_3$ ; 3 $\text{m}^2/\text{gm}$	1294	1.032	1.057	+2.42
	1127	0.989	1.010	+2.12
2. AP Specific Surface = 5393 $\text{cm}^2/\text{gm}$	783	0.873	0.877	+0.46
	532	0.718	0.721	+0.42
Blend of 400- $\mu$ and 10- $\mu$ AP Particles	1290	1.037	1.056	+1.83
	1012	0.973	0.972	-0.10
	446	0.672	0.643	-4.32

**TABLE A-3**  
**(Continued)**

Formulation	Pressure, psia	Burn Rate at 77 F, in./sec		$\Delta$ r, %
		Experimental	Calculated	
LCA-8911X-3	1784	1.087	1.062	-2.30
1. 0.4% $\text{Fe}_2\text{O}_3$ ; 9.4 $\text{m}^2/\text{gm}$	1141	0.911	0.924	+1.43
	990	0.810	0.880	+8.64
2. AP Specific Surface	655	0.716	0.741	+3.49
= 5284 $\text{cm}^2/\text{gm}$	403	0.546	0.556	+1.83
Blend of 400- $\mu$ and 10- $\mu$	2012	1.135	1.100	-3.08
AP Particles	1344	0.964	0.975	+1.14
	1106	0.881	0.915	+3.86
LCA-8904X-2	1393	0.696	0.784	-12.64
1. 0.5 % $\text{Fe}_2\text{O}_3$ ; 26.4 $\text{m}^2/\text{gm}$	2104	0.855	0.915	+ 7.02
	1360	0.701	0.777	+10.84
2. AP Specific Surface	982	0.622	0.683	+9.81
= 3985 $\text{cm}^2/\text{gm}$	725	0.551	0.601	+9.07
Blend of 200- $\mu$ and 10- $\mu$	399	0.418	0.453	+8.57
AP Particles	241	0.318	0.334	+5.05
LCA-8904Y-3	803	0.611	0.617	+0.98
1. 0.5 % $\text{Fe}_2\text{O}_3$ ; 3.9 $\text{m}^2/\text{gm}$	472	0.479	0.486	+1.46
	1133	0.715	0.709	-0.84
2. 1% $\text{Fe}_2\text{O}_3$ ; 5.1 $\text{m}^2/\text{gm}$	1031	0.682	0.683	+0.15
	601	0.552	0.544	-1.45
3. AP Specific Surface	346	0.423	0.413	-2.36
= 4010 $\text{cm}^2/\text{gm}$	1541	0.791	0.797	+0.76
Blend of 200- $\mu$ and 10- $\mu$	2008	0.896	0.879	-1.90
AP Particles				
LCA-8908X-2	1365	0.480	0.479	-0.21
1. 1% $\text{Fe}_2\text{O}_3$ ; 5.1 $\text{m}^2/\text{gm}$	2130	0.551	0.550	-0.18
	1224	0.464	0.463	-0.22
2. AP Specific Surface	1310	0.470	0.473	+0.64
= 1520 $\text{cm}^2/\text{gm}$	1036	0.441	0.439	-0.45
	803	0.405	0.403	-0.49
Blend of 400- $\mu$ , 200- $\mu$	714	0.385	0.386	+0.26
and 10- $\mu$ AP Particles	544	0.349	0.349	0.00
LCA-8906X-2	1685	0.857	0.812	-5.25
1. 1% $\text{Fe}_2\text{O}_3$ ; 9.2 $\text{m}^2/\text{gm}$	1374	0.786	0.753	-4.20
	1242	0.752	0.725	-3.59
2. AP Specific Surface	801	0.635	0.609	-4.09
= 3985 $\text{cm}^2/\text{gm}$	685	0.600	0.570	-5.00
Blend of 200- $\mu$ and 10- $\mu$	2148	0.962	0.888	-7.69
AP Particles	953	0.682	0.654	-4.11



TABLE A-5  
(Continued)

Formulation	Pressure, psia	Burn Rate at 77 F. in./sec		$\Delta r, \%$
		Experimental	Calculated	
LCA-8909Y-5	495	0.329	0.334	-1.52
1. 1.5% $Fe_2O_3$ ; 5 $m^2/gm$	747	0.390	0.390	0.00
	859	0.413	0.409	-0.97
2. AP Specific Surface	982	0.436	0.428	-1.83
= 1550 $cm^2/gm$	1323	0.472	0.471	-0.21
Blend of 400- $\mu$ , 200- $\mu$	1892	0.531	0.526	-0.94
and 10- $\mu$ AP Particles	460	0.325	0.324	-0.31
LCA-8908-1	1979	0.564	0.553	-1.95
1. 1.5% $Fe_2O_3$ ; 5.1 $m^2/gm$	851	0.424	0.421	-0.71
	1553	0.490	0.490	0.00
2. AP Specific Surface	1077	0.468	0.456	-2.56
= 1550 $cm^2/gm$	406	0.313	0.316	+0.96
Blend of 400- $\mu$ , 200- $\mu$	723	0.402	0.397	-1.24
and 10- $\mu$ AP Particles	594	0.373	0.370	-0.80
	306	0.276	0.275	-0.36
LCA-8908Y-3	531	0.356	0.357	+0.28
1. 1% $Fe_2O_3$ ; 9.4 $m^2/gm$	781	0.413	0.413	0.00
	875	0.429	0.430	+0.23
2. AP Specific Surface	1965	0.552	0.559	+1.27
= 1520 $cm^2/gm$	1579	0.495	0.500	+1.00
Blend of 400- $\mu$ , 200- $\mu$	1089	0.459	0.463	+0.87
and 10- $\mu$ AP Particles				
LCA-8909-1	1855	0.534	0.532	-0.37
1. 1.5% $Fe_2O_3$ ; 3.9 $m^2/gm$	827	0.412	0.410	-0.49
	1538	0.485	0.480	-1.03
2. AP Specific Surface	1050	0.446	0.444	-0.45
= 1550 $cm^2/gm$	585	0.303	0.304	+0.33
Blend of 400- $\mu$ , 200- $\mu$	292	0.270	0.265	-1.85
and 10- $\mu$ AP Particles	569	0.358	0.358	0.00
	727	0.414	0.392	-5.31
LCA-8909A-2	585	0.299	0.303	+1.34
1. 1.5% $Fe_2O_3$ ; 3.7 $m^2/gm$	728	0.341	0.347	+1.76
	782	0.393	0.401	+2.04
2. AP Specific Surface	985	0.430	0.434	+0.93
= 1550 $cm^2/gm$	1229	0.462	0.466	+0.88
Blend of 400- $\mu$ , 200- $\mu$	1810	0.527	0.526	-0.19
and 10- $\mu$ AP Particles	647	0.363	0.375	+3.31
	320	0.274	0.277	+1.09

TABLE A-3  
(Continued)

Formulation	Pressure, psia	Burn Rate at 77 F, in./sec		$\Delta r, \%$
		Experimental	Calculated	
LCA-8904-1	1906	0.938	0.948	+1.07
1. 1% $\text{Fe}_2\text{O}_3$ ; 26.4 $\text{m}^2/\text{gm}$	921	0.698	0.707	+1.29
	1321	0.828	0.820	-0.90
2. AP Specific Surface	1228	0.814	0.796	-2.21
= 3985 $\text{cm}^2/\text{gm}$	663	0.608	0.611	+0.49
Blend of 200- $\mu$ and 10- $\mu$	508	0.534	0.538	+0.75
AP Particles	436	0.479	0.497	-3.76
	307	0.424	0.407	-4.01
LCA-8906-1	1649	0.847	0.799	-5.67
1. 1% $\text{Fe}_2\text{O}_3$ ; 8.4 $\text{m}^2/\text{gm}$	493	0.508	0.488	-3.94
	876	0.640	0.627	-2.03
2. AP Specific Surface	294	0.394	0.370	-6.09
= 3985 $\text{cm}^2/\text{gm}$	1426	0.783	0.757	-3.32
Blend of 200- $\mu$ and 10- $\mu$	956	0.681	0.649	-4.70
AP Particles	607	0.550	0.537	-2.36
LCA-8905-1	1493	0.714	0.714	0.00
1. 1% $\text{Fe}_2\text{O}_3$ ; 3.9 $\text{m}^2/\text{gm}$	704	0.543	0.538	-0.92
	394	0.410	0.403	+0.73
2. AP Specific Surface	1666	0.737	0.742	+0.68
= 3985 $\text{cm}^2/\text{gm}$	1181	0.649	0.656	+1.08
Blend of 200- $\mu$ and 10- $\mu$	827	0.572	0.574	+0.35
AP Particles	796	0.567	0.565	-0.35
	495	0.463	0.461	-0.43

TABLE A-4  
COMPARISON OF CALCULATED AND EXPERIMENTAL BURN RATES  
OF  $\text{Fe}_2\text{O}_3$ -CATALYZED CTPB PROPELLANTS  
(Regression Analysis Index of Determination = 0.992)  
(Mean  $1/r = 2.114487$ ;  $\sigma$  (est) = 0.0704)

Formulation	Pressure, psia	Burn Rate at 77 F, in./sec		$\Delta r, \%$
		Experimental	Calculated	
LCA-8933-2	1617	0.611	0.622	+2.13
1. 1% $\text{Fe}_2\text{O}_3$ ; 5.1 $\text{m}^2/\text{gm}$	1510	0.595	0.604	+1.51
2. AP Specific Surface	1213	0.534	0.544	+1.87
- 2422 $\text{cm}^2/\text{gm}$	1087	0.504	0.517	+2.51
Blend of 200- $\mu$ and	856	0.453	0.460	-1.55
7-11- $\mu$ AP Particles	620	0.396	0.393	-0.76
LCA-8934-1	839	0.519	0.504	-2.89
1. 1% $\text{Fe}_2\text{O}_3$ ; 9.2 $\text{m}^2/\text{gm}$	1532	0.678	0.676	-0.29
2. AP Specific Surface	1388	0.634	0.644	+1.58
- 2787 $\text{cm}^2/\text{gm}$	1108	0.576	0.578	+0.35
Blend of 200- $\mu$ and	2097	0.778	0.785	+0.90
7-11- $\mu$ AP Particles	1296	0.613	0.623	+1.63
LCA-8935-1	2114	0.824	0.790	-4.13
1. 1% $\text{Fe}_2\text{O}_3$ ; 5.1 $\text{m}^2/\text{gm}$	1721	0.747	0.720	-3.61
2. AP Specific Surface	1633	0.739	0.707	-4.33
- 3163 $\text{cm}^2/\text{gm}$	1540	0.723	0.684	-5.39
Blend of 200- $\mu$ and	1206	0.640	0.612	-4.38
7-11- $\mu$ AP Particles	1008	0.590	0.563	-4.58
LCA-8936-1	1909	0.857	0.844	-1.52
1. 1% $\text{Fe}_2\text{O}_3$ ; 9.2 $\text{m}^2/\text{gm}$	1787	0.836	0.820	-1.91
2. AP Specific Surface	1292	0.707	0.710	+0.42
- 3634 $\text{cm}^2/\text{gm}$	1138	0.673	0.671	-0.30
Blend 200- $\mu$ and	777	0.575	0.564	-1.91
7-11- $\mu$ AP Particles	827	0.583	0.580	-0.51
LCA-8934-1	797	0.703	0.666	-5.26
1. 1% $\text{Fe}_2\text{O}_3$ ; 9.2 $\text{m}^2/\text{gm}$	1074	0.802	0.771	-3.87
2. AP Specific Surface	1098	0.803	0.779	-2.92
- 5599 $\text{cm}^2/\text{gm}$	1536	0.920	0.916	-0.43
Blend of 200- $\mu$ and	394	0.484	0.461	-4.75
10- $\mu$ AP Particles	1575	0.938	0.927	-1.17
	428	0.504	0.482	-4.37
	836	0.737	0.682	-7.46
	1361	0.875	0.864	-1.26



TABLE A-4  
(Continued)

Formulation	Pressure, psia	Burn Rate at 77 F., in./sec		$\Delta r, \%$
		Experimental	Calculated	
LCA-8955-1	685	0.580	0.589	+1.55
1. 1% $\text{Fe}_2\text{O}_3$ ; 5.1 $\text{m}^2/\text{gm}$	1079	0.703	0.734	-4.41
2. AP Specific Surface	637	0.555	0.569	+2.52
= 5599 $\text{cm}^2/\text{gm}$	1151	0.757	0.721	+4.99
Blend of 200- $\mu$ and 10- $\mu$	1200	0.772	0.727	+6.19
AP Particles	1560	0.873	0.827	-5.56
	1986	0.976	0.946	+3.17
	325	0.399	0.388	+2.84
LCA-8967-1	395	0.340	0.346	-1.76
1. 0.1% $\text{Fe}_2\text{O}_3$ ; 26.4 $\text{m}^2/\text{gm}$	479	0.362	0.381	+5.25
2. AP Specific Surface	625	0.401	0.433	+7.98
= 3196 $\text{cm}^2/\text{gm}$	201	0.242	0.246	+1.65
Blend of 200- $\mu$ and	995	0.498	0.537	+7.83
7-11- $\mu$ AP Particles	1946	0.695	0.725	+4.52
	684	0.422	0.452	+7.11
LCA-8968-1	1795	0.647	0.605	-6.49
1. 0.1% $\text{Fe}_2\text{O}_3$ ; 5.1 $\text{m}^2/\text{gm}$	395	0.329	0.309	-6.08
2. AP Specific Surface	1015	0.489	0.476	-2.66
= 3196 $\text{cm}^2/\text{gm}$	600	0.393	0.377	-4.07
Blend of 200- $\mu$ and	658	0.406	0.393	-3.20
7-11- $\mu$ AP Particles	965	0.476	0.465	-2.51
	524	0.373	0.354	-5.09
LCA-8969-1	757	0.484	0.495	+2.27
1. 0.2% $\text{Fe}_2\text{O}_3$ ; 10 $\text{m}^2/\text{gm}$	540	0.419	0.430	+2.63
2. AP Specific Surface	458	0.392	0.398	+1.55
= 5559 $\text{cm}^2/\text{gm}$	244	0.292	0.294	-0.68
Blend of 200- $\mu$ and 7-11- $\mu$	2279	0.827	0.797	-3.65
AP Particles	822	0.504	0.519	+2.98
	1177	0.596	0.605	+1.51
LCA-8969X-2	777	0.495	0.500	+1.01
1. 0.2% $\text{Fe}_2\text{O}_3$ ; 8.4 $\text{m}^2/\text{gm}$	202	0.265	0.263	-0.75
2. AP Specific Surface	575	0.439	0.437	-0.46
= 5559 $\text{cm}^2/\text{gm}$	2589	0.864	0.799	-3.05
Blend of 200- $\mu$ and 7-11- $\mu$	1219	0.620	0.605	-2.42
AP Particles	859	0.518	0.522	+0.77
	480	0.404	0.402	-0.50

TABLE A-4  
(Continued)

Formulation	Pressure, psia	Burn Rate at 77 F., in./sec		$\Delta r, \%$
		Experimental	Calculated	
LCA-8970-1	643	0.412	0.404	-1.94
1. 0.6% $\text{Fe}_2\text{O}_3$ ; 9.2 $\text{m}^2/\text{gm}$	780	0.443	0.444	+0.23
2. AP Specific Surface	1018	0.497	0.506	-1.81
= 2440 $\text{cm}^2/\text{gm}$	390	0.332	0.314	-5.42
Blend of 200- $\mu$ and 7-11- $\mu$	531	0.376	0.367	-2.39
AP Particles	2210	0.726	0.731	+0.69
	1068	0.509	0.518	+1.77
LCA-8981-1*	521	0.427	0.434	+1.64
1. 0.4% $\text{Fe}_2\text{O}_3$ ; 3 $\text{m}^2/\text{gm}$	795	0.520	0.530	-1.92
2. AP Specific Surface	180	0.247	0.248	-0.40
= 4715 $\text{cm}^2/\text{gm}$	565	0.451	0.451	0.00
Blend of 200- $\mu$ and 10- $\mu$	1242	0.637	0.647	-1.57
AP Particles	907	0.544	0.563	-3.49
LCA-8971-1	371	0.296	0.296	0.00
1. 0.3% $\text{Fe}_2\text{O}_3$ ; 3.7 $\text{m}^2/\text{gm}$	433	0.320	0.319	-0.31
2. AP Specific Surface	548	0.346	0.358	-3.47
= 2821 $\text{cm}^2/\text{gm}$	884	0.430	0.448	-4.19
Blend of 200- $\mu$ and 7-11- $\mu$	868	0.427	0.444	-3.98
AP Particles	1707	0.594	0.601	-1.18
	587	0.360	0.369	+2.50
LCA-8975-1	1457	0.498	0.476	-4.42
1. 0.3% $\text{Fe}_2\text{O}_3$ ; 5.1 $\text{m}^2/\text{gm}$	766	0.368	0.360	-2.17
2. AP Specific Surface	485	0.300	0.295	-1.67
= 1520 $\text{cm}^2/\text{gm}$	439	0.285	0.283	-0.70
Blend of 200- $\mu$ and 7-11- $\mu$	325	0.249	0.250	+0.40
AP Particles	1850	0.541	0.524	-3.14
LCA-8977-1	444	0.288	0.296	+2.78
1. 0.1% $\text{Fe}_2\text{O}_3$ ; 26.4 $\text{m}^2/\text{gm}$	506	0.304	0.313	-2.96
2. AP Specific Surface	738	0.361	0.369	+2.22
= 1517 $\text{cm}^2/\text{gm}$	1365	0.466	0.482	-3.45
Blend of 200- $\mu$ and 7-11- $\mu$	447	0.290	0.296	+2.07
AP Particles	1795	0.517	0.542	+4.84

\* A coarse 10- $\mu$  of 9500  $\text{cm}^2/\text{gm}$  was used in this mix.



Rocketdyne Division  
Rockwell International

TABLE A-4  
(Continued)

Formulation	Pressure, psia	Burn Rate at 77 F, in./sec		$\Delta r, \%$
		Experimental	Calculated	
LCA-8978-1	567	0.366	0.360	-1.64
1. 1% $\text{Fe}_2\text{O}_3$ 9.4 $\text{m}^2/\text{gm}$	642	0.389	0.381	-2.06
	897	0.448	0.443	-1.12
2. AP Specific Surface	1591	0.571	0.571	0.00
= 1532 $\text{cm}^2/\text{gm}$	331	0.288	0.285	-1.04
Blend of 200- $\mu$ and	867	0.441	0.436	-1.13
7-11- $\mu$ AP Particles	1879	0.621	0.614	-1.13